AD-A161 994 LASER-INDUCED KINETICS: AN EXPERIMENTAL AND THEORETICAL PROGRAM(U) SRI INTERNATIONAL MENLO PARK CA N SELAMOGLU ET AL 25 OCT 85 AFOSR-TR-85-1097 1/1

UNCLASSIFIED F49620-83-K-0001 F/G 7/5 NL

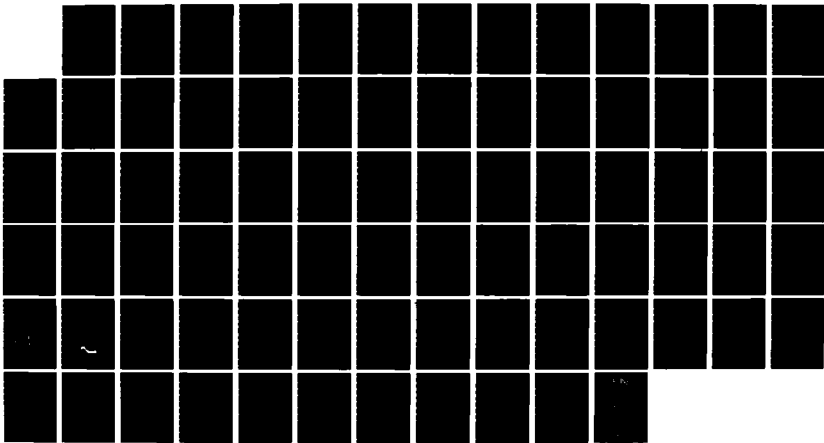

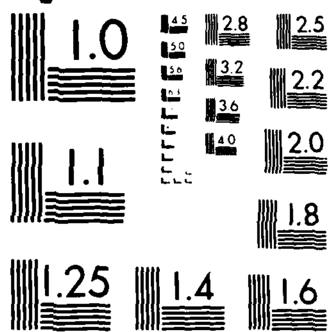

MICROCOPY RESOLUTION TEST CHART
NATIONAL BUREAU OF STANDARDS 1963 A

AD-A161 994

SRI International

AFOSR TR- 7

October 25, 1985

Final Report

Covering the period: 01 October 1982 to 30 September 1985

LASER-INDUCED KINETICS:
AN EXPERIMENTAL AND THEORETICAL PROGRAM

By: N. Selamoglu, M. J. Rossi, and D. M. Golden

Prepared for:

Directorate of Chemical Sciences (NC)
AIR FORCE OFFICE OF SCIENTIFIC RESEARCH (AFOSR)
Bolling Air Force Base, Building 410
Washington, DC 20332

Attention: Dr. Donald L. Ball, Director

SRI Research Project PYU-4917
AFOSR Contract No. F49620-83-K-0001

Approved:

D. C. Lorents, Laboratory Director
Chemical Physics Laboratory

G. R. Abrahamson
Vice President
Physical Sciences Division

DTIC FILE COPY

333 Ravenswood Ave • Menlo Park CA 94025
415 326-6200 • TWX 910-373-2046 • Telex 334 486

85 12 6 069

UNCLASSIFIED
SECURITY CLASSIFICATION OF THIS PAGE

AD-A161994

REPORT DOCUMENTATION PAGE

1a. REPORT SECURITY CLASSIFICATION: UNCLASSIFIED

1b. RESTRICTIVE MARKINGS: N/A

2a. SECURITY CLASSIFICATION AUTHORITY: N/A

2b. DECLASSIFICATION/DOWNGRADING SCHEDULE: N/A

3. DISTRIBUTION/AVAILABILITY OF REPORT: Approved for public release, distribution unlimited

4. PERFORMING ORGANIZATION REPORT NUMBER(S): SRI International PYU-4917

5. MONITORING ORGANIZATION REPORT NUMBER(S): AFOSR-TR- 1097

6a. NAME OF PERFORMING ORGANIZATION: SRI International

6b. OFFICE SYMBOL (If applicable)

7a. NAME OF MONITORING ORGANIZATION: Air Force Office of Scientific Research

6c. ADDRESS (City, State and ZIP Code)
333 Ravenswood Avenue
Menlo Park, CA 94025

7b. ADDRESS (City, State and ZIP Code)
Bolling Air Force Base, Bldg. 410, DC 20332

8a. NAME OF FUNDING/SPONSORING ORGANIZATION: AFOSR

8b. OFFICE SYMBOL (If applicable): NC

9. PROCUREMENT INSTRUMENT IDENTIFICATION NUMBER: Contract No. F49620-83-K-0001

8c. ADDRESS (City, State and ZIP Code)
Directorate of Chemical Sciences (NC)
Bolling Air Force Base, Bldg. 410
DC 20332

10. SOURCE OF FUNDING NOS.

PROGRAM ELEMENT NO.	PROJECT NO.	TASK NO.	WORK UNIT NO.
----	2303	B1	----

11. TITLE (Include Security Classification): LASER-INDUCED KINETICS: An Experimental and Theoretical Program

12. PERSONAL AUTHOR(S): N. SELAMOGLU, M. J. ROSSI, AND D. M. GOLDEN

13a. TYPE OF REPORT: FINAL

13b. TIME COVERED: FROM 1 OCT 82 TO 30 SEPT 85

14. DATE OF REPORT (Yr., Mo., Day): 1985 OCTOBER 25

15. PAGE COUNT: 78

16. SUPPLEMENTARY NOTATION

17. COSATI CODES

FIELD	GROUP	SUB. GR.

18. SUBJECT TERMS (Continue on reverse if necessary and identify by block number)
VLPØ very low-pressure pyrolysis
Laser-induced Kinetics
Radical-Surface Chemistry

19. ABSTRACT (Continue on reverse if necessary and identify by block number)

The kinetics of CF_3 and CH_3 radical reactions have been investigated using the VLPØ method. The reactions of interest were radical recombination and metathetical halogenation (Br_2, Cl_2). In addition to yielding gas-phase reaction rates, these studies pointed out the importance of gas-surface interactions in the chemistry. The VLPØ technique was also used to investigate a radical-surface reaction: the reaction of CF_3 radicals on a silicon oxide surface. The latter study revealed that H_2O on the surface plays a major role in the chemistry. The surface reaction was studied as functions of surface temperature (320-530 K) and CF_3 concentration.

20. DISTRIBUTION/AVAILABILITY OF ABSTRACT: UNCLASSIFIED/UNLIMITED ☒ SAME AS RPT. ☐ DTIC USERS ☐

21. ABSTRACT SECURITY CLASSIFICATION: UNCLASSIFIED

22a. NAME OF RESPONSIBLE INDIVIDUAL: F. J. Wodarczyk

22b. TELEPHONE NUMBER (Include Area Code): 767-4963

22c. OFFICE SYMBOL: NC

DD FORM 1473, 83 APR — EDITION OF 1 JAN 73 IS OBSOLETE.

UNCLASSIFIED
SECURITY CLASSIFICATION OF THIS PAGE

I. SUMMARY

The original goal of this research program was to measure absolute rate constants for fast radical reactions over a range of temperatures using the VLPΦ (Very Low Pressure Photolysis) technique. The reactions of interest include radical recombination and metathetical halogenation reactions of CF_3 and CH_3, and other radicals. For reasons summarized below we have redirected our studies to radical-surface interactions. The latter are of considerable interest from the viewpoint of semiconductor processing. Our studies throughout the duration of the project are outlined below and detailed in the appendices.

A. Gas Phase Chemistry

As detailed in our earlier annual reports, the VLPΦ technique was used to study the following reactions:

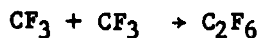

$$CF_3 + CF_3 \rightarrow C_2F_6$$

$$CF_3 + Br_2 \rightarrow CF_3Br + Br$$

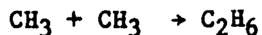

$$CH_3 + CH_3 \rightarrow C_2H_6$$

$$CH_3 + Br_2 \rightarrow CH_3Br + Br$$

$$CH_3 + Cl_2 \rightarrow CH_3Cl + Cl$$

Although rate constants were determined for all of the reactions, these had large error bars and were not always reproducible. Complications arose

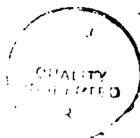

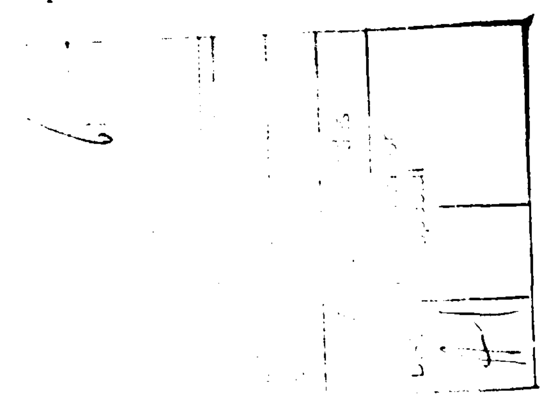

because of complex gas-surface interactions on the reactor walls competing with the homogeneous gas-phase chemistry of interest. Three types of walls were tested: uncoated Pyrex walls, and Teflon-coated or halocarbon-wax-coated walls. The coatings proved to undergo irreversible changes over the course of several experiments. Furthermore, we found that varying the temperature leads to irreversible changes on the surface coating. These difficulties led to high errors in the data, making it difficult to determine rate constants with good precision for a given temperature, or to determine weak temperature dependences as would be expected for the reactions above (see Appendix A for details).

B. Radical-Surface Chemistry

Following the above study we directed our attention to investigating gas-surface interactions. We have examined the reaction of CF_3 radicals on fused silica, SiO_2. Whether or not CF_3 radicals etch SiO_2, and the rate of such a reaction is of great interest from the viewpoint of plasma etching. Our results showed that indeed CF_3 undergoes reaction on the SiO_2 surface, but that only a small part of the surface reaction is accounted for by the etching of SiO_2. The major reaction of CF_3 is with H_2O present on the surface, leading to mostly CO and HF. Under these conditions very little etching of the SiO_2 occurred, as seen from the small yields of volatile product SiF_4. The order and the temperature dependence of the H_2O-initiated reaction was investigated. It was found to be first order with respect to $[CF_3]$ and strongly temperature-dependent. Our measurements also led to a determination of the sticking coefficient of CF_3 on the SiO_2 surface as a function of temperature. We are currently continuing the study,

this time observing the surface reaction under conditions where H_2O is absent (details in Appendix B).

C. CF_3-CF_3 Gas-Phase Recombination

In the $SiO_2 + CF_3$ study it was necessary to take into account the homogeneous recombination of CF_3 radicals, which is competitive with the surface chemistry. This recombination rate was measured under the conditions discussed in part B but in the absence of an active surface, giving $k_r = 3.0 \times 10^{-12}$ cm^3 s^{-1} at room temperature. Besides complementing study B, our rate constant is a contribution to the values in the literature, which range from 5×10^{-12} to 4×10^{-11} (see Appendix C for details). Our present measurement of k_r has better precision than our earlier determination in part A; however, the values agree reasonably well (3×10^{-12} versus 5×10^{-12}). The main differences between the two approaches are the following: A was under non steady-state conditions where the product concentration was followed as a function of time (a single pulse from the CO_2-laser-generated radicals), whereas C was under near-steady-state conditions where steady-state product yields were monitored (the laser was at a high pulse repetition rate). The latter approach appears to facilitate the determination of reaction rates. The other difference between cases A and C was that the reactor in C was gold-coated rather than Teflon- or halocarbon wax-coated as in A. The gold-coated surface appears to be inert with respect to CF_3 adsorption and provides consistently reproducible results, unlike the other coatings. Overall, method C seems a better choice for the determination of reaction rates. In the future, we plan to measure various radical reaction rates in this way.

II. PUBLICATIONS

See Appendices B and C for manuscripts submitted for publication.

III. PERSONNEL

The professional personnel associated with this research effort are:

David M. Golden, Director, Department of Chemical Kinetics

Michel J. Rossi, Chemist (Ph.D)

Nur Selamoglu, Research Associate (Ph.D)

John R. Barker, Chemist (Ph.D.)--until March 1985.

IV. PAPERS PRESENTED AT MEETINGS AND CONFERENCES

David M. Golden	University of Paris, VI 30 October 1984 to 30 January 1985 Series of lectures (partially supported by AFOSR funds)
	XII Int'l Conference on Photochemistry Tokyo, Japan 04-09 August 1985
Michel J. Rossi	AFOSR Contractors' Meeting Albuquerque, New Mexico 23-28 October 1984
	International Conference on Chemical Kinetics NBS, Gaithersburg, MD 16-20 June 1985
	AVS Surface/Interface Research Meeting Palo Alto, CA 17 July 1985
Nur Selamoglu	International Symposium on Gas Kinetics, Nottingham, England 16-20 July 1984
	AVS Surface/Interface Research Meeting, Palo Alto, CA 17 July 1985

V. CONSULTATIVE AND ADVISORY FUNCTION TO OTHER LABORATORIES AND AGENCIES

None.

VI. NEW DISCOVERIES, INVENTIONS, OR PATENT DISCLOSURESs

None.

Appendix A

2nd ANNUAL REPORT, AFOSR Contract No. F49620-83-K-0001

(Covering the period: 1 October 1983 thru 30 September 1984)

SRI International

April 25, 1985

Annual Report
Covering the Period: 1 October 1983 thru
30 September 1984

LASER-INDUCED KINETICS: AN EXPERIMENTAL AND THEORETICAL PROGRAM

By: N. Selamoglu, M. J. Rossi,
and D. M. Golden

Prepared for:

Directorate of Chemical Sciences (NC)
AIR FORCE OFFICE OF SCIENTIFIC RESEARCH (AFOSR)
Bolling Air Force Base, Building 410
Washington, DC 20332

Attention: Dr. Donald L. Ball, Director

SRI Research Project PYU-4917
AFOSR Contract No. F49620-83-K-0001

Approved:

Donald C. Lorents, Laboratory Director
Chemical Physics Laboratory

G. R. Abrahamson
Vice President
Physical Sciences Division

ABSTRACT

The reactions

$$2CF_3 \rightarrow C_2F_6$$

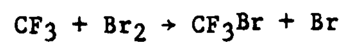

$$CF_3 + Br_2 \rightarrow CF_3Br + Br$$

$$2CH_3 \rightarrow C_2H_6$$

$$CH_3 + Br_2 \rightarrow CH_3Br + Br$$

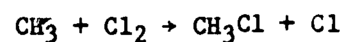

$$CH_3 + Cl_2 \rightarrow CH_3Cl + Cl$$

have been studied by the very low-pressure photolysis (VLPΦ) method. The radicals are generated from precursor molecules by IRMPD. It has been found that gas-surface interactions play an important role in the chemistry.

CONTENTS

ABSTRACT ii

LIST OF ILLUSTRATIONS.. iv

INTRODUCTION... 1

REACTIONS OF CF_3 RADICALS..................................... 2
Method of Approach... 2
CF_3-CF_3 Recombination.. 3
CF_3 + Br_2 Reactions.. 8

REACTIONS OF METHYL RADICALS................................... 11
CH_3-CH_3 Recombination.. 11
CH_3 + Br_2 and CH_3 + Cl_2 Reactions.......................... 13

DISCUSSION... 16

REFERENCES... 17

ILLUSTRATIONS

1	Relative C_2F_6 Yield as a Function of CF_3I Flow Rate for Teflon-Coated Cell at 300 K...........................	4
2	Relative C_2F_6 Yield as a Function of CF_3I Flow Rate for Uncoated Pyrex Cell at 300 K..........................	5
3	Relative CF_3Br and C_2F_6 Yields as Functions of Br_2 Flow Rate for Teflon-Coated Cell at 300 K..................	9
4	C_2H_6 Yield as a Function of $[CH_3]_o$ at 300 K................	12
5	CH_3Br Yield as a Function of $[Br_2]$ at 300 K...............	14

INTRODUCTION

The goal of this research program is the measurement of fast absolute rate constants for radical reactions using the VLPΦ method. The reactions of interest are radical-halogen metathetical reactions and radical-radical recombinations. Specifically, this reporting period we concluded our study on CF_3 radical reactions and also investigated the reactions of CH_3 radicals with bromine and chlorine. This report summarizes the results of these experiments.

REACTIONS OF CF_3 RADICALS

Originally, we planned to use the VLPΦ mewthod to study the temperature dependence of rate constants for CF_3 reactions: reaction with bromine and CF_3-CF_3 recombination. However, we found that various surface effects compete with gas-phase processes of interest and make it difficult to extract meaningful rate data. In an effort to find an inert surface, we used three types of wall coatings in the photolysis cell: Teflon, halocarbon wax, and Pyrex. Below we discuss the general method of approach, then present the results.

Method of Approach

In a VLPΦ reactor the chemical reactions of interest are in competition with escape of reactants out of the cell. The overall mechanism for these may be written as

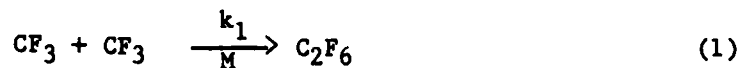

$$CF_3 + CF_3 \xrightarrow[M]{k_1} C_2F_6 \quad (1)$$

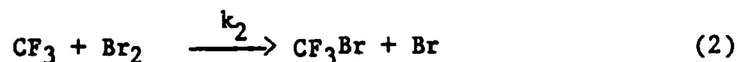

$$CF_3 + Br_2 \xrightarrow{k_2} CF_3Br + Br \quad (2)$$

$$CF_3 \xrightarrow{k_3} \text{escape out of reactor} \quad (3)$$

In addition, first-order wall losses may occur, for example:

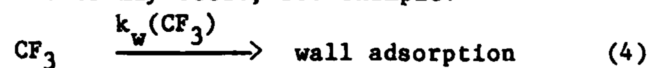

$$CF_3 \xrightarrow{k_w(CF_3)} \text{wall adsorption} \quad (4)$$

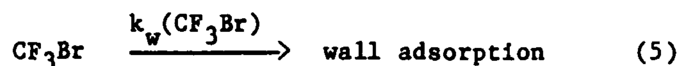

$$CF_3Br \xrightarrow{k_w(CF_3Br)} \text{wall adsorption} \quad (5)$$

Integrated C_2F_6 and CF_3Br yields for the above scheme (1-3) may be expressed as follows:

$$Y(C_2F_6) = V \cdot \tfrac{1}{2}\left([CF_3]_o - \frac{k_3 + k_2[Br_2]}{k_1} \ln\left(\frac{k_3 + k_2[Br_2] + k_1[CF_3]_o}{k_3 + k_2\,[Br_2]}\right)\right) \quad (6)$$

$$Y(CF_3Br) = V \cdot \frac{k_2}{k_1} [Br_2] \ln\left(\frac{k_3 + k_2 [Br_2] + k_1[CF_3]_o}{k_3 + k_2[Br_2]}\right) \qquad (7)$$

where V is the reactor volume, $[CF_3]_o$ is the initial CF_3 concentration (i.e., immediately following the dissociation of the CF_3I precursor), and $[Br_2]$ is the steady-state concentration of Br_2. The above expressions are based on the assumption that $[Br_2]$ remains constant during reaction, a condition that is met by using excess Br_2. For the reactor used in our experiments, V is 135 cm^3, and the escape rate constants are given by: $k_3(S) = 0.675\ (T/M)^{1/2}$, $k_3(L) = 1.827\ (T/M)^{1/2}$, where T(K) and M(g/mol) refer, respectively, to the temperature and the molecular weight. The expressions (6-7) may be modified to accommodate the wall losses (4-5).

In our experiments, C_2F_6 and CF_3Br yields were followed as functions of $[CF_3]_o$ and $[Br_2]$. Rate constants were estimated by fitting these data to expressions such as (6) and (7), which were modified to include possible wall losses. In some cases, the yields could not be expressed analytically (for example, when $[Br_2]$ did not remain constant), so numerical methods were used.

CF_3-CF_3 Recombination

We first studied reaction (1) in the absence of Br_2. Figure 1 shows representative results of the relative yield of C_2F_6 versus CF_3I flow rate for a Teflon-coated reactor at 300 K. Notice that the experimental data approach the limiting value of 1.0 with increasing CF_3I flow rate, indicating that the available CF_3 radicals are all being converted to C_2F_6. This is expected since, as the CF_3 concentration is increased (i.e., CF_3I flow rate is increased), second-order reaction (1) will dominate over first-order CF_3 escape (reaction 3). The curvature of the plot at the lower flow rates, where escape and reaction are competitive, determines the value of k_1. The curves shown in Figure 1 are model curves obtained by using $k_1 = 5 \times 10^{-12}$ $cm^3\ s^{-1}$ and the appropriate escape rate constants in expression (6). The model provides a good fit to the experimental data with no indication of wall losses. The uncertainty in this k_1 determination was about ± 20%.

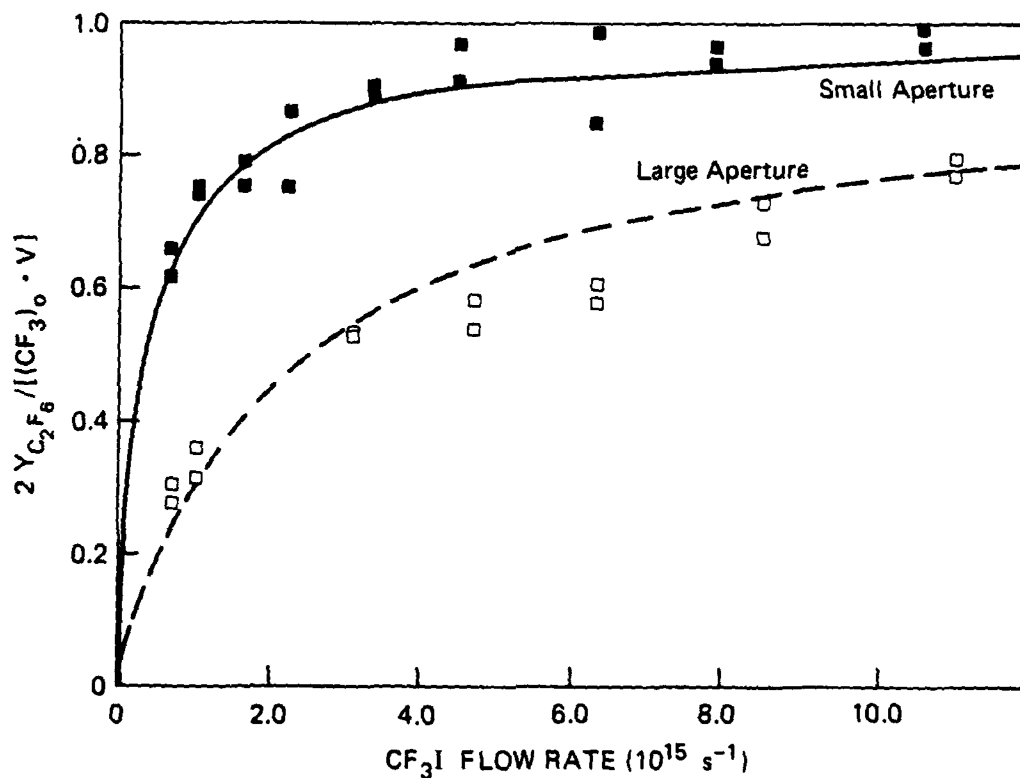

FIGURE 1 RELATIVE C_2F_6 YIELD AS A FUNCTION OF CF_3I FLOW RATE FOR TEFLON-COATED CELL AT 300 K

Model curves are for $k_1 = 5 \times 10^{-12}$ cm^3 s^{-1} and $k_w(CF_3) = 0$ s^{-1}. CF_3I flow rate of 12×10^{15} s^{-1} corresponds to $[CF_3]_0 = 1.45 \times 10^{13}$ and 5.33×10^{12} cm^{-3} for the small and large apertures, respectively.

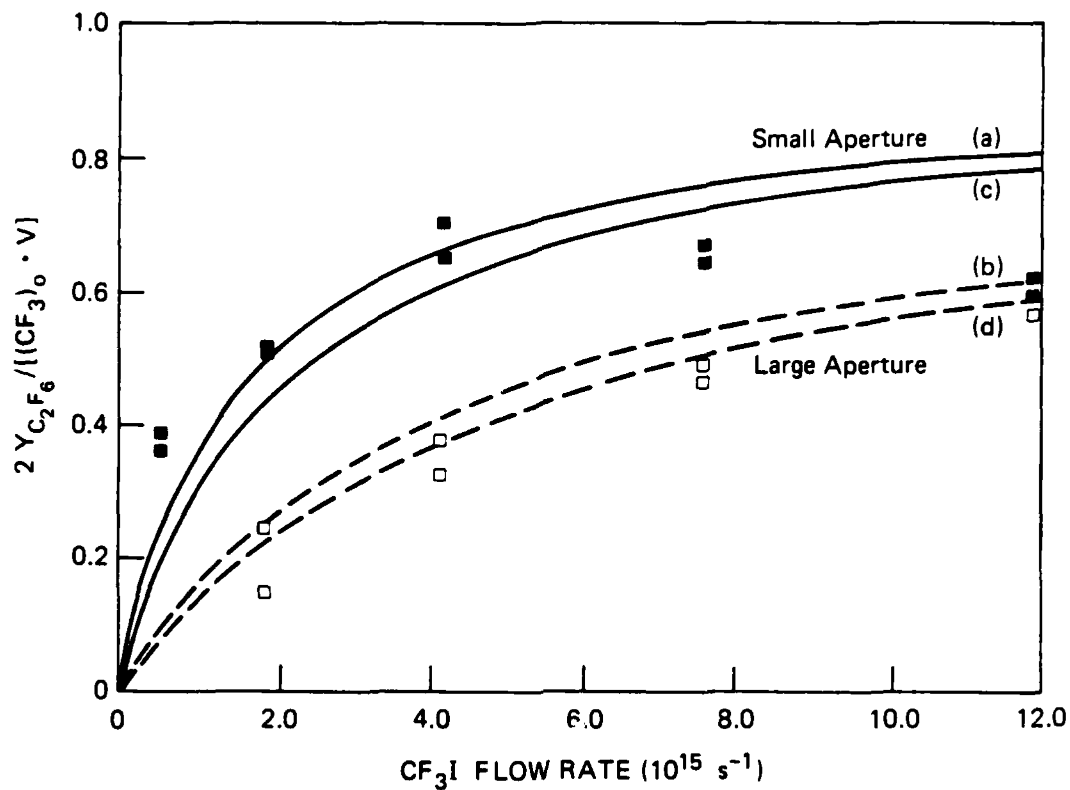

FIGURE 2 RELATIVE C_2F_6 YIELD AS A FUNCTION OF CF_3I FLOW RATE FOR UNCOATED PYREX CELL AT 300 K

The upper and lower curves for each aperture correspond to two sets of rate constants in the model:
a,b: $k_1 = 5 \times 10^{-12}$ cm^3 s^{-1}, $k_w(CF_3) = 7$ s^{-1}.
c,d: $k_1 = 10 \times 10^{-12}$ cm^3 s^{-1}, $k_w(CF_3) = 20$ s^{-1}.

Table 1

CF_3-CF_3 RECOMBINATION*

Expt. No.	Wall	T, K	k_1, $cm^2\ s^{-1}$		$k_w(CF_3)$, s^{-1}	Remarks
1	Teflon	300	$5(\pm 1) \times 10^{-12}$		0	No apparent wall loss; newly coated cells.
2	Halocarbon wax	300	$5(\pm 1) \times 10^{-12}$		0	
3	Pyrex	300	5×10^{-12}	and	7	It is necessary to include wall loss in the mechanisms; however, it does not seem to be simple first order.
				or		
			10×10^{-12}	and	20	
4	Teflon	385	$4(\pm 1) \times 10^{-12}$		3	
5	Teflon	235	- - -		- -	Scatter and complexity of data do not allow determination of rate constants.
6	Halocarbon wax	267	5×10^{-12}	and	5	C_2H_6 deficiency at high flow rates. Neither set of rate constants fit the data very well.
				or		
			2×10^{-12}	and	0	
7	Pyrex	230	- - -		- -	Only 50% of the decomposed CF_3I can be recovered. Lacks variation of C_2F_6 yield with CF_3I flow.

---

*

- Laser fluence = 2.3 J cm^{-2} (1076 cm^{-1}).
- Decomposition per pulse of CF_3I in cell volume = 13%, corresponding to 50% decomposition in the irradiated volume.
- V_{cell} = 135 cm^3
- The escape rate constants for the cell are given by:

  small aperture: $0.675\ (T/M)^{1/2}$
  large aperture: $1.827\ (T/M)^{1/2}$

  where T is the temperature (K) and M is the molecular weight (g/mol).

For comparison, we studied the same reaction in an uncoated Pyrex vessel. The results are shown in Figure 2. In the Pyrex vessel the C_2F_6 yield does not approach the limiting value of 1.0. We attribute this C_2F_6 deficiency to wall loss of CF_3. However, the results could not be fitted with a first-order or a second-order heterogeneous CF_3 loss, and we conclude that it may be a complex mixed-order process. Model curves with first-order $k_w(CF_3)$ are shown in Figure 2 to emphasize the difficulty in obtaining k_1 values from such data.

Table 1 summarizes the results obtained for CF_3-CF_3 recombination under different temperature and reactor wall conditions. From most of these measurements, useful rate constant information for homogeneous CF_3 reactions could not be obtained, mainly because of experimental uncertainties in conjunction with wall effects, which often led to irreproducible results. However, the results were interesting and are summarized below:

- Newly coated Teflon and halocarbon wax were both satisfactory at 300 K. These new coatings resulted in no apparent wall losses, and both yielded $k_1 = 5 \times 10^{-12}$.

- As the Teflon and wax coatings aged, they led to substantial CF_3 losses, similar to the losses that occurred when uncoated Pyrex walls were used.

- Increasing or decreasing the temperature from 300 K both resulted in an increase in the apparent CF_3 loss (Teflon coating). This effect cannot be ascribed directly to temperature, however, because it may also arise from irreversible changes in the surface properties of the coating.

- The higher temperature (385 K) experiments were performed using only the Teflon coating. These yielded $k_1 = 4(\pm 1) \times 10^{-12}$ with $k_w(CF_3) = 3\ s^{-1}$. Within experimental error, k_1 is unchanged from its room temperature value. In fact, k_1 is not expected to change much over such a small temperature range,[1] so any change in C_2F_6 yield can be ascribed to the onset of heterogeneous CF_3 loss processes.

- For all three types of walls, the lower temperatures (230-270 K) caused greater wall problems than room temperature. These low temperature data were not useful for determining k_1 because of experimental errors and/or complexity of the data.

- Note that although our value of $k_1 = 5 \times 10^{-12}$ at 300 K is in excellent agreement with that calculated by Rossi and Golden, it is inconsistent with results of earlier experiments on CF_3 in which C_2F_6 was not observed as a product.[2] This indicated that recombination must occur on the surface and that the wall conditions were different in the two experiments.

$CF_3 + Br_2$ Reaction

Having examined reaction (1) under various conditions, we performed experiments in which Br_2 was present to obtain the rate constant of reaction (2) as a function of temperature. In addition to the wall problems associated with CF_3, using Br_2 introduced another wall loss--that of the CF_3Br product. Although it is unusual to attribute a heterogeneous loss to a stable compound such as CF_3Br, this represents the simplest mechanism that fits our experimental data.

In these experiments, the CF_3I flow rate was kept constant, and the CF_3Br and C_2F_6 yields were measured as functions of Br_2 flow rate. Two wall types were used: Teflon at 300 and 385 K and halocarbon wax at 267 and 300 K. Figure 3 shows a representative data set for the Teflon reactor at room temperature. Notice that, as expected, increasing Br_2 flow rate results in increasing CF_3Br and decreasing C_2F_6 yields. The CF_3Br yield does not approach the limiting value of 1.0, however, and the data could not be fitted using only a CF_3 wall loss in the model. The data in Figure 3 are fitted very well by $k_2 = 1.0 \times 10^{-12}$ and $k_w(CF_3Br) = 0.5\ s^{-1}$, whereas the corresponding fit to the large-aperture data is poor. Within our reaction scheme, it was not possible to establish rate constants that fit both small- and large-aperture data sets, indicating that the reaction mechanism is more complex than outlined in equations (1-5). Values for k_1 and $k_w(CF_3)$ in these analyses were taken directly from the corresponding entry in Table 1.

Table 2 summarizes the results for the $CF_3 + Br_2$ experiments. In all cases, there was difficulty in fitting the data because of the many variable parameters. Only the halocarbon wax data at 300 K could be fitted well with $k_2 = 1.0 \times 10^{-12}$ and $k_w(CF_3Br) = 0.3\ s^{-1}$. For the other

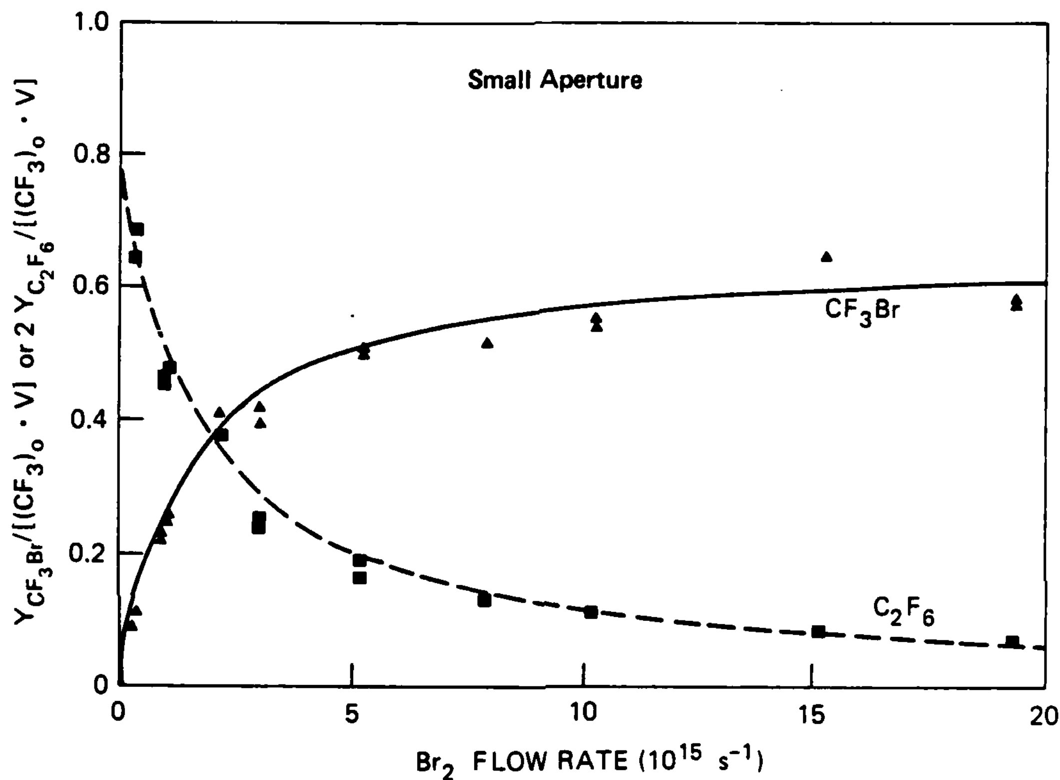

FIGURE 3 RELATIVE CF_3Br AND C_2F_6 YIELDS AS FUNCTIONS OF Br_2 FLOW RATE FOR TEFLON-COATED CELL AT 300 K

Only small aperture data are shown.
CF_3I flow rate = $2.2 \times 10^{15}\ s^{-1}$ ($[CF_3]_o = 2.6 \times 10^{12}\ cm^{-3}$).
A Br_2 flow rate of $2.0 \times 10^{16}\ s^{-1}$ corresponds to $[Br_2] = 1.7 \times 10^{14}\ cm^{-3}$.
Model rate constants are $k_1 = 5 \times 10^{-12}\ cm^3\ s^{-1}$;
$k_2 = 1.0 \times 1.0^{-12}\ cm^3\ s^{-1}$; $k_w(CF_3) = 0\ s^{-1}$; $k_w(CF_3Br) = 0.5\ s^{-1}$.

Table 2

EXPERIMENTS FOR $CF_3 + Br_2$ REACTION
(Irradiation conditions given in Table 1)

Exp. No.	Wall	T, K	k_2 $cm^3\ s^{-1}$	$k_w(CF_3Br)$, s^{-1}	Remarks
1	Teflon	300	- - -	$k_w > 0.5$ probably	Both large and small aperture data sets cannot be fitted simultaneously
2	Teflon	385	- - -	$k_w > 0.5$ probably	
3	Halocarbon wax	300	1×10^{-12}	0.3	For $k_1 = 5 \times 10^{-12}$, $k_w(CF_3) = 0$.
4	Halocarbon wax	267	1×10^{-12}	and 0.1	For $k_1 = 5 \times 10^{-12}$, $k_w(CF_3) = 5$.
				or	
			0.4×10^{-12}	and 0.2	For $k_1 = 2 \times 10^{-12}$, $k_w(CF_3) = 0$.

temperatures and for the Teflon coating, there were inconsistencies in fitting both small- and large-aperture data. Our value of k_2 (for halocarbon wax) agrees with earlier measurements of 1.3×10^{-12} ($\pm$ 0.2).[2]

In conclusion, our results emphasize the difficulty in obtaining the rate information of interest because of wall problems. It is especially difficult to determine the temperature dependence for a given reaction because all the processes in scheme (1-5) are expected to be temperature dependent to varied extents.

REACTIONS OF METHYL RADICALS

From reports in the literature, methyl halogenation reactions appeared to be interesting candidates for study by the VLPΦ method. The methyl radical precursor was pentafluoroanisol (PFA), dissociated by CO_2 laser excitation. PFA had been successfully used by others for this purpose.[3,4]

We studied the following methyl radical reactions at 300 K in a Pyrex cell:

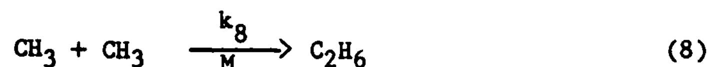

$$CH_3 + CH_3 \xrightarrow[M]{k_8} C_2H_6 \qquad (8)$$

$$CH_3 + Br_2 \xrightarrow{k_9} CH_3Br + Br \qquad (9)$$

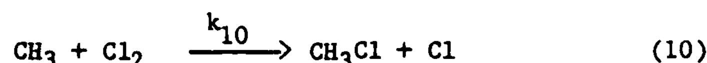

$$CH_3 + Cl_2 \xrightarrow{k_{10}} CH_3Cl + Cl \qquad (10)$$

The reaction scheme is similar to that presented in the previous sections for CF_3 (equations 1-5), and expressions similar to (6) and (7) are applicable.

Literature values for k_{10} range from 3×10^{-13} to 1.5×10^{-12}, whereas k_9 was measured to be 2×10^{-11}.[5] A comparative study[6] indicates that $(k_{10}/k_9) = 0.028 \pm 0.015$.

CH_3-CH_3 Recombination

As in the case of CF_3, we first obtained measurements to characterize the CH_3-CH_3 recombination reaction within our VLPΦ reactor (silanized Pyrex surface). Figure 4 shows our experimental data in a slightly different format than the earlier CF_3 data; absolute C_2H_6 yields are shown as functions of $[CH_3]_o$, together with model curves. It is interesting that the data do not follow the general curvature of the model, regardless of the value of k_8 used in the model. The fit could not be improved by introducing reasonable values for first-order wall losses. We concluded that there were possibilities of complex wall-loss effects, as well as wall-catalyzed CH_3 recombination.

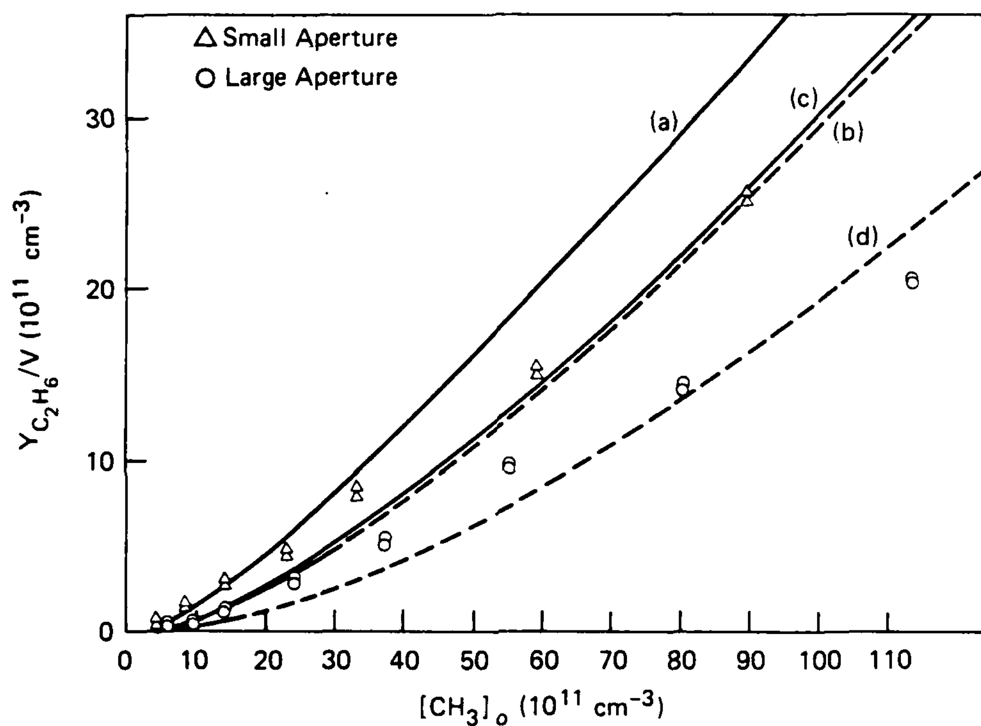

FIGURE 4 C_2H_6 YIELD AS A FUNCTION OF $[CH_3]_o$ AT 300 K
a,b Model with $k_8 = 1.6 \times 10^{-12}$ cm^3 s^{-1}
c,d Model with $k_8 = 0.6 \times 10^{-12}$ cm^3 s^{-1}
$[CH_3]_o = 100 \times 10^{11}$ cm^{-3} corresponds to a PFA flow rate of 3.8×10^{15} and 1.0×10^{16} s^{-1} for the small and large apertures, respectively.

However, despite the poor fit between model and experiment, notice that the data are encompassed between two extremes for k_8 (0.6 to 1.6 x 10^{-12}). We chose to use these as "operational" values for k_8 in order to account for recombination in further experiments. Under our conditions, the homogeneous gas-phase rate constant is expected to be between 1.5 x 10^{-12} and 1.5 x 10^{-11} (estimated f om falloff curves using k_∞ and k_o). Our experimental k_8 = 1 x 10^{-12} is rather close to the lower calculated value. Despite this apparent agreement, the question whether or not surface recombination plays a role remains unanswered because of uncertainties in both the measured and estimated values. In fact, in the VLPΦ Knudsen cell, where gas-wall collisions compete with gas-phase collisions and the low-pressure limit of the rate constant is determined by the gas-wall collision frequency, it would be surprising if recombination were not "surface-assisted" to some degree.

CH_3 + Br_2 and CF_3 + Cl_2 Reactions

The experiments with CH_3 + Br_2 and CF_3 + Cl_2 were similar to the CF_3 + Br_2 experiments described above. Results for CH_3 + Br_2 are shown in Figure 5 as CH_3Br yields versus [Br_2]. Notice that, using the upper value for k_8 (1.6 x 10^{-12}, see previous section) and with k_9 = 2 x 10^{-11}, the large aperture data can be fitted rather well (curve a), whereas the corresponding small-aperture results are overestimated (curve b). In contrast, using the lower value for k_8(0.6 x 10^{-12}) and with k_9 = 4 x 10^{-12}, we obtain a good fit to the small-aperture data (curve c), and the large-aperture data are underestimated (curve d). Introducing various wall losses did not improve the fitting. Thus, the small- and large-aperture data sets cannot be fitted simultaneously using our simple reaction mechanism. In addition, both sets of rate constants in the model overestimate the C_2H_6 yields (not shown in Figure 5) by a factor of 5 to 7. All these results indicate that the mechanisms are complex and not represented by our simple scheme.

Our results for CH_3 + Cl_2 showed trends similar to those for the bromination case. Upper and lower limits for k_{10} were found to be 2 x 10^{-12} and 0.7 x 10^{-12}, respectively. These data also did not allow for simultaneous fitting of CH_3Cl yields for the two apertures. The C_2H_6 yields, however, were somewhat better predicted by the model.

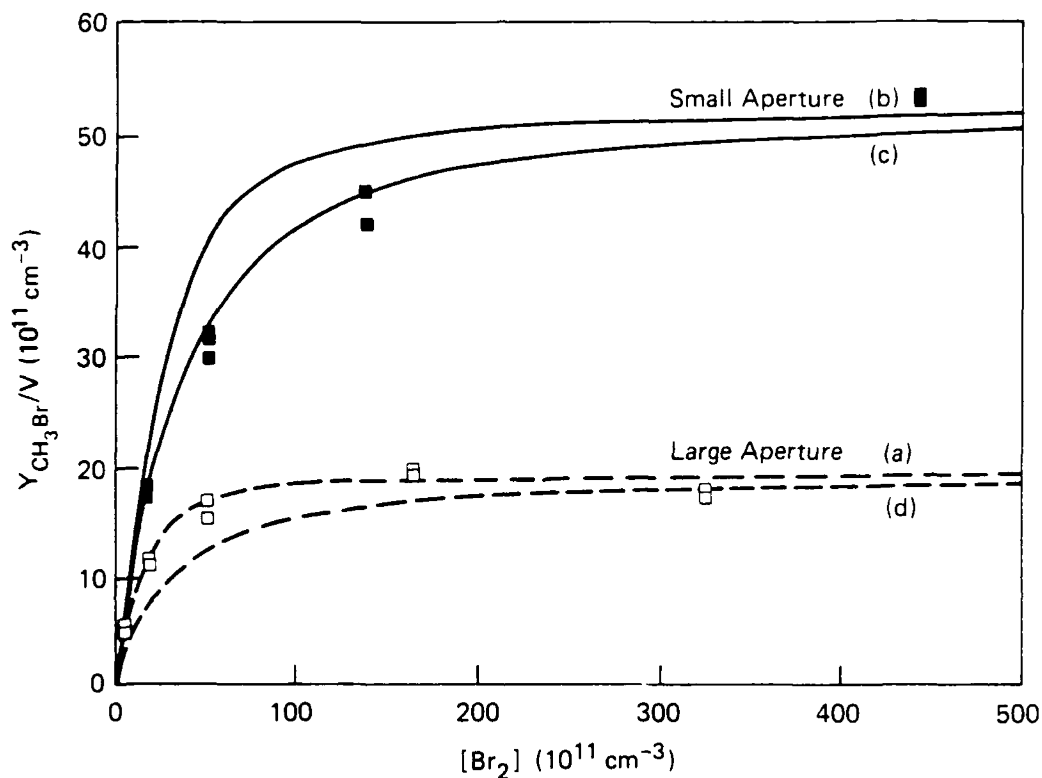

FIGURE 5 CH_3Br YIELD AS A FUNCTION OF $[Br_2]$ at 300 K

a,b Model with $k_8 = 1.6 \times 10^{-12}$ cm^{-3} s^{-1}, $k_9 = 2 \times 10^{-11}$ cm^{-3} s^{-1}.
c,d Model with $k_8 = 0.6 \times 10^{-12}$ cm^{-3} s^{-1}, $k_9 = 4 \times 10^{-12}$ cm^{-3} s^{-1}.
PFA flow rate = 2.0×10^{15} s^{-1} ($[CH_3]_o = 5.4 \times 10^{12}$ cm^{-3} for the small aperture and 2.0×10^{12} cm^{-3} for the large aperture).
$[Br_2] = 500 \times 10^{11}$ cm^{-3} corresponds to Br_2 flow rates of 6.2×10^{15} and 1.7×10^{16} s^{-1} for the small and large apertures, respectively.

Table 3 summarizes the results for the CH_3 reactions and lists the "upper" and "lower" limits for k_8, k_9 and k_{10}. It is interesting that our values for k_9 and k_{10} are near those from the literature quoted earlier.

Table 3

METHYL RADICAL REACTIONS*

Reaction		Rate Constant, $cm^3\ s^{-1}$
$CH_3 + CH_3$	k_8	$0.6 \times 10^{-12} - 1.6 \times 10^{-12}$
$CH_3 + Br_2$	k_9	$4.0 \times 10^{-12} - 2.0 \times 10^{-11}$
$CH_3 + Cl_2$	k_{10}	$0.7 \times 10^{-12} - 2.0 \times 10^{-12}$

*Laser fluence = 2.7 J cm^{-2} (1041 cm^{-1}). Dissociation of PFA in cell volume is 30 -35%, corresponding to ~100% decomposition in the irradiated volume. The cell volume and escape rate constants are given in Table 1.

DISCUSSION

Our methyl radical experiments indicate problems similar to those in the CF_3 studies. In both, surface effects play an important role. As we did for CF_3, it may be useful to study the methyl reactions for a variety of wall coatings.

In addition to wall effects, we observed another problem in the CH_3 experiments. The precursor PFA appears not to be a straightforward source of methyl radicals. Besides methyl, we found an abundance of another product with mass 28. This is probably CO, perhaps from secondary photodissocation of the pentafluorophenoxy radical. It is not clear whether such by-products played a role in the chemistry we were studying. We decided to discontinue use of PFA as a methyl source. Better alternatives are CH_3-N_2-CH_3 or CH_3I in conjunction with UV excimer laser excitation, and we plan to come back to this system in the future.

Our studies show the importance of gas-surface interactions in the VLPΦ method. This result is not surprising because in the Knudsen cell, reactants undergo $\sim 10^4$ to 10^5 wall collisions before they react or escape. Therefore, it is important to use inert walls when studying homogeneous gas-phase reactions. On the other hand, these interactions between the walls and the gas suggest that the VLPϕ technique may be useful to study heterogeneous gas-surface reactions instead.

REFERENCES

1. M. Rossi and D. M. Golden, Int. J. Chem. Kinetics, 11, 775 (1979).

2. M. J. Rossi, J. R. Barker, and D. M. Golden, J. Chem. Phys., 71, 3722 (1979).

3. F. Yamada, I. R. Slagle, and D. Gutman, Chem. Phys. Lett., 83, 409 (1981).

4. J. A. McCaulley, S. M. Anderson, J. B. Jeffries, and F. Kaufman, Chem. Phys. Lett., 115, 180 (1985).

5. L. J. Kovalenko and S. R. Leone, J. Chem. Phys., 80, 3656 (1984), and references therein.

6. B. S. Evans and E. Whittle, Int. J. Chem. Kinetics, 10, 745 (1978).

Appendix B

REACTION OF CF_3 RADICALS ON FUSED SILICA BETWEEN 320-530 K

By: N. Selamoglu, M. J. Rossi, and D. M. Golden

Accepted by The Journal of Chemical Physics

REACTION OF CF_3 RADICALS ON FUSED SILICA BETWEEN 320-530K[†]

N. Selamoglu,[*] M. J. Rossi, and D. M. Golden
Department of Chemical Kinetics
SRI International, Menlo Park, CA 94025

ABSTRACT

The reaction between CF_3 radicals and silicon oxide (fused silica) surface was studied in a VLPΦ flow reactor (~ 0.1-3 mTorr) as functions of surface temperature (320-530K) and CF_3 concentration. The CF_3 radicals were generated from CF_3I by CO_2 laser photolysis, and the subsequent gas-phase reaction products were followed by mass spectroscopy. The surface reaction was found to yield CO, HF, CO_2, COF_2 and SiF_4. It was found that H_2O residing on the silicon oxide surface was largely responsible for the oxygen- and hydrogen-containing products, and that little etching of the SiO_2 itself occurred under these conditions. The rates for the irreversible surface loss of CF_3 , and for the formation of CO were both first order with respect to $[CF_3]$. These were found to be temperature dependent with $E_a \simeq 4.7$ kcal/mol and 7.5 kcal/mol, respectively. The CF_3 surface loss rate indicates that the sticking coefficient for this radical on quartz is between 0.0014-0.017 for the temperature range of this study.

[†]This work was supported by the Air Force Office of Scientific Research, Contract No. F49620-83-K-0001.

[*]Postdoctoral Research Associate.

CK85-28

INTRODUCTION

In the plasma etching of semiconductor materials, it is known that neutrals as well as charged species play roles in the etching process.[1-3] Neutrals, such as atoms and radicals, etch the substance of interest isotropically while ion bombardment produces anisotropic etching. In general, the etching process must involve the following: chemical adsorption of the active species on the surface, rearrangement of the reactant-surface intermediate to yield etch products, and the removal of volatile etch products from the surface by desorption. Ion bombardment may assist neutral etching in various ways, such as by preparing a clean surface prior to the adsorption step, or by desorbing products from the surface, as well as possibly affecting the chemistry.

The extreme complexity of plasma systems involving atoms, radicals, ions, and electrons makes it difficult to extract fundamental mechanistic information on the process. In order to assess the importance of various neutral and ionic reactions, model experiments must be carried out under controlled conditions. Among these are studies where atoms or radicals are generated either photochemically or by a discharge, and then reacted with the surface of interest[4-8] as well as beam studies on ion-surface interactions.[9,10] The etching of silicon and silicon oxide by F-atoms has been studied extensively,[4-7] and it has been found that F-atoms selectively and efficiently etch silicon. In the etching of silicon oxide, however, fluorocarbon radicals, such as CF_2 and CF_3, are expected to play an important role, according to results from plasma etching studies. The reactivities of CF_2 and

CF_3 radicals with Si and SiO_2 have been studied under non-ionic conditions where the surfaces of interest were irradiated with the same UV excimer laser beam generating the radicals.[4,8] In these high pressure (10-500 torr) studies, it was found that CF_2 etches SiO_2 efficiently while CF_3 has poor efficiency.

The motivation for the present study was to fill a gap between various studies ranging from complex plasma systems to ultra-high vacuum beam studies. The purpose was to investigate the reactivity of CF_3 on a fused silica surface at pressures and radical concentrations resembling those in plasma etchers ($\leq$ 10 mtorr total pressure, 10^{11}-10^{13} radicals cm^{-3}). Unlike in beam studies of ion-surface interactions, the substrate was not intended to be a well-characterized clean surface but rather be under conditions of "practical" interest. In this work, a CO_2 laser beam was used to generate radicals but not to irradiate the surface. The surface temperature could be varied between 25-300°C.

The VLPΦ (very low-pressure photolysis) method used for this investigation is a well-established technique[11-13] for the kinetic study of homogeneous gas-phase reactions and is used here for the first time to study radical-surface interactions. (Variations in which radicals were generated via microwave discharge have been used in the past.[14]) Due to the importance of gas-wall collisions inherent in the method, it is almost always necessary to deactivate the vessel walls when studying homogeneous gas-phase processes. This disadvantage from the viewpoint of gas-phase chemistry makes it possible to study gas-surface chemistry by VLPΦ. In the latter, the vessel

walls are again deactivated, but this time, the active surface of interest is placed in the vessel and exposed to the reactant. Reactants and products are monitored mass spectrometrically.

The method yields not only qualitative information on the gas-phase product spectrum but also quantitative information on reaction rates. The latter include the rate of consumption of CF_3 radicals on the silica surface and the rates of formation of products as functions of the surface temperature. These data allow the determination of CF_3 sticking coefficients on fused silica as functions of temperature.

EXPERIMENTAL

The VLPΦ technique utilizes a low-pressure (< 10 mtorr) Knudsen flow reactor, where molecular flow conditions are maintained. The reactor used in our measurements is shown in Figure 1. The radical precursor CF_3I flows into the Knudsen cell where it resides for 1.7 seconds, before it effuses out of the exit aperture and into the mass spectrometric detection area. Decomposition to form CF_3 is effected by a CO_2 laser. The fate of the CF_3 radicals is then either to recombine, yielding C_2F_6, or to escape from the reactor. The collision number of 1.3×10^4 with the reactor walls ensures thermalization of the CF_3 radicals before any of the above reactions take place. In the event that an active surface is present in the cell, as is the case in this study, CF_3 may also undergo gas-surface reaction during the time it strikes that surface. (The collision number for the active surface is 600 s^{-1}.) The gas-phase products leaving the reactor are formed into an effusive molecular beam which is monitored mass spectrometrically, and the rates of the chemical reactions are obtained with respect to the known escape rate. The VLPΦ method may be carried out under steady-state or under single-pulse irradiation conditions. In this particular study, a high repetition rate (20 Hz) laser was used: since the time between pulses is shorter than the residence time or typical times for reaction (seconds), species' concentrations are maintained at close to steady-state conditions.

The processes involving CF_3 in the VLPΦ reactor are summarized in the following scheme.

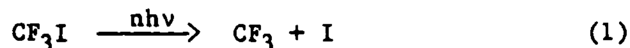

$$CF_3I \xrightarrow{nh\nu} CF_3 + I \qquad (1)$$

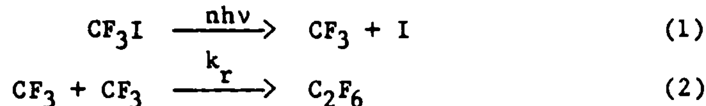

$$CF_3 + CF_3 \xrightarrow{k_r} C_2F_6 \qquad (2)$$

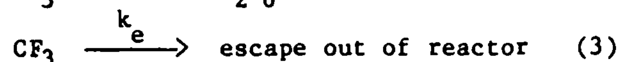

$$CF_3 \xrightarrow{k_e} \text{escape out of reactor} \qquad (3)$$

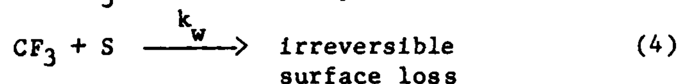

$$CF_3 + S \xrightarrow{k_w} \text{irreversible surface loss} \qquad (4)$$

Step (1) represents the IR-laser multiphoton decomposition forming CF_3 while (2) is the homogeneous gas-phase recombination[15] forming C_2F_6. Loss of CF_3 other than by recombination include escape (3) and surface reaction (4).

Under steady-state conditions the above mechanism leads to the following expression:

$$f(F^{i}_{CF_3I})/(F^{o}_{C_2F_6}) = 2 + (k_e + k_w)k_r^{-1/2}V^{1/2}\, {F^{o}_{C_2F_6}}^{-1/2} \qquad (5)$$

where $F^{i}_{CF_3I}$ is the flow rate of CF_3I into the reactor, $F^{o}_{C_2F_6}$ is the C_2F_6 flow rate out of the reactor, V is the volume and f is the fractional depletion in the steady-state CF_3I signal when the sample is irradiated. Thus, with the appropriate measurements of $F^{i}_{CF_3I}$, f, and $F^{o}_{C_2F_6}$, in conjunction with the known k_e and k_r, the CF_3 surface loss rate constant k_w may be obtained.

In fact, two methods were used to generate the CF_3 radicals from the CF_3I precursor: (a) CO_2 Laser IR-Multiphoton Decomposition and the (b) Hot Wire Decomposition. The laser experiments led to quantitative kinetic studies. The hot-wire experiments were designed to obtain qualitative information on

the origin of products. A hot nichrome wire (800–1000°C) effected CF_3I decomposition in the latter experiments.

Experiments consisted of flowing CF_3I through the reactor and measuring steady-state mass spectrometric signals of CF_3I and of stable gas-phase reaction products. These were followed with laser on/off, as functions of CF_3I flow rate and of substrate temperature.

The parameters for the VLPΦ reactor are: $V = 250\ cm^3$; reactor wall area = $420\ cm^2$; IR-beam pathlength = 10 cm. The escape rate constant for species with molecular weight, M, is given by $k_e(M) = 0.475 \left(\frac{T}{M}\right)^{1/2}$. The pyrex reactor was gold-coated (Engelhard Industries) to minimize wall losses. The fused silica substrate (2-inch diameter) rested on a heated stainless-steel block in the wafer compartment, and its temperature was monitored using a thermocouple.

A Tachisto 555 CO_2 laser was used with the following irradiation conditions: $\bar{\nu} = 1076\ cm^{-1}$ (9.6 R(16) line), pulse repetition rate = 20 Hz, beam diameter = 1.1 cm, fluence = $0.8\ J/cm^2$; fractional dissociation per pulse in irradiated volume = 3–12%.

The molecular beam effusing from the cell was chopped by means of a tuning fork chopper and analyzed using a Balzers 311 quadrupole mass spectrometer. The technique discriminates against all background gases not originating from the cell. Mass spectral calibrations of signal versus flow rate were carried out for all the compounds of interest.

RESULTS AND DISCUSSION

A. Origin of Products

Typical experimental traces of the mass spectrometric signal of reactant and products, with laser on/off are shown in Figure 2. The observable gas-phase products from the reaction of CF_3 with fused silica are CO, HF, CO_2, COF_2 and SiF_4, in decreasing order of importance. In fact, the CO and HF are approximately 25-100 times larger in quantity than the other products. SiF_4 is the least important, about 100 times less than CO. These products all come from a surface reaction on the fused silica. The actual yields are not exactly reproducible over several weeks' measurements, however, general trends are reproducible. This is attributed to changing conditions on the surface. In addition to the surface reaction products there is the competing gas-phase recombination product C_2F_6. All of the products are observed only in the presence of CF_3I and with laser irradiation, thus ruling out the possibility of CF_3I undergoing dissociative adsorption on the surface. (This is equivalent to a CF_3I sticking coefficient, γ, of less than 10^{-5} given our detection sensitivity.)

The origin of HF has to be elucidated first, since neither the reactant nor the substrate compositions contain any hydrogen. Another question concerns the balance of Si versus O in the reaction products. The only Si-containing product SiF_4 occurs in quantities $\sim$ 100-200 times smaller than the O-containing products CO, CO_2,COF_2, most of which is comprised by CO. If the oxygen in CO were coming directly from SiO_2, then we would expect much more SiF_4 than observed to make up the balance, because SiF_4 was the only Si-containing product under our experimental conditions.

In all of our mass spectra, we noticed the presence of H_2O in the cell background. The H_2O is independent of the laser and of the CF_3I flow, but may show some variation from day-to-day. We believe the water originates

from the bulk glass, i.e., the silica substrate and the Pyrex reactor. The mass spectral signals indicate apparent H_2O flow rates between 10^{14} and 10^{15} s^{-1}, depending on the substrate temperature. In hot-wire experiments with CF_3I, we noticed that the heating of the wire and the formation of HF was accompanied by a noticeable decrease in the H_2O, suggesting that the source of HF was H_2O. This was clarified by experiments whe[illegible] $_2O$ was deliberately flowed into the cell, ($F^i_{D_2O}$ = 3 x 10^{15} s^{-1}, $F^i_{CF_3I}$ = 1.1 x 10^{15} s^{-1}) . As expected, DF was seen in appreciable quantities (F^o_{DF} ~ 8 x 10^{14} s^{-1}), confirming that the origin of HF was indeed H_2O. The fact that the flux of HF or DF out of the Knudsen cell is small can be attributed to the well-known tendency of HF to physisorb to glass and metal surfaces. Once the source of HF is turned off, the flux lingers on for hours so that HF cannot be used as a probe for the surface reaction in a convenient way.

In addition to producing DF, the presence of D_2O affected the other products. CO showed a factor of 1.7 increase, while SiF_4 decreased by a factor of ~ 3, as did C_2F_6 (see Figure 3). That CO increases in the presence of D_2O suggests that some of the CO may originate from water. We shall address this question below with oxygen-isotope measurements. The decrease in SiF_4 with D_2O may come about because (1) the SiF_4 product reacts with D_2O, or (2) in the presence of D_2O, there is less CF_3 available for the etching reaction to produce SiF_4, due to reaction of CF_3 with D_2O. Under our conditions, possibility (1) is not important. Control experiments were carried out with small flow rates of SiF_4 and H_2O at various substrate temperatures. The SiF_4 signal did not show any dependence on the presence of water. Explanation (2) accounts for the depletion in SiF_4: The SiO_2 and the surface H_2O compete against each other for reaction with CF_3. When H_2O or D_2O is present, there is less available CF_3 for the SiO_2 etching reaction

thereby decreasing SiF_4. Since there is less CF_3 available for the recombination reaction as well, we see a decrease also in the C_2F_6 yield when water is present (Figure 3c). Thus, the etching reaction is inhibited by the presence of water.

Next, H_2O^{18} experiments were performed in order to find the source of oxygen in the O-containing products CO, CO_2 and COF_2, the two possible sources being SiO_2 and H_2O. Labeled H_2O^{18} was flowed through the reactor for several hours and allowed to equilibriate before measurement. The mass spectrum of the products revealed the presence of all isotopic combinations: CO^{18}, $CO_2{}^{18}$, $CO^{18}O^{16}$, and $CO^{18}F_2$ appeared while CO^{16}, $CO_2{}^{16}$, and $CO^{16}F_2$ remained mostly unchanged. The quantitative results are shown in Table I. Notice that the abundance of each isotopic composition agrees with the H_2O^{18}/H_2O^{16} ratio. In the case of CO_2, where two oxygens are present, the $CO_2{}^{16}$: $CO^{18}O^{16}$: $CO_2{}^{18}$ ratios follow the probability rule $(H_2O^{16})^2$: $2(H_2O^{16} * H_2O^{18})$: $(H_2O^{18})^2$ very well.

The good agreement between the product ratios and the H_2O^{18}/H_2O^{16} ratio indicates that almost all of the CO, CO_2, and COF_2 come from the reaction of CF_3 with water, and that the contribution from $CF_3 + SiO_2$ is very small indeed. Furthermore, if the latter had been important, a considerable amount of SiF_4 would have to be expected in order to account for the silicon. Since we have very little SiF_4 in our measurements, this supports the conclusion that the SiO_2 etching reaction is not as important as the $CF_3 + H_2O$ reaction under our conditions. It should be emphasized that while the majority of the reaction is traced to water, this is a surface reaction consuming CF_3 and occurring on the fused silica surface, because the reaction products are only observable when CF_3 radicals strike the heated surface.

B. Kinetics

Figures 4, 5, and 6 show product concentrations as functions of $[CF_3]_o$ for the laser experiments. $[CF_3]_o$ is the steady-state CF_3 concentration that would be available if there were no chemical losses [given by $(f * F^{i}_{CF_3I}) / (V * k_e)$]. Notice that all products show positive dependence on the CF_3 concentration. Notice in Figures 4 and 5 that for a given $[CF_3]_o$, increasing temperature affects $[C_2F_6]$ and [CO] in different ways. CO, representative of the surface reaction, increases with temperature while C_2F_6 decreases. This suggests that at the higher surface temperatures the rates for the surface reactions increase, thereby throttling off the gas-phase recombination reaction. The other surface-related products, CO_2, COF_2, and SiF_4 show temperature dependence similar to CO (not shown in figure).

The temperature dependence may be seen more clearly in Figure 7 showing the dependence of the reaction products on substrate temperature with constant CF_3I flow rate. Notice the strong increase in surface-related products CO, CO_2, HF, SiF_4, and COF_2 with temperature. We associate the increased yields of the surface-related products with strongly temperature-dependent surface-reaction rates. The decrease in the surface product COF_2 at the high temperatures is attributable to decomposition of that product following its formation on the surface. By contrast, the decrease in the C_2F_6 yield at the higher temperatures is ascribed to a competition effect: the strongly temperature-dependent surface reaction competes against the nearly temperature independent gas-phase recombination for the available CF_3 radicals, thereby decreasing the C_2F_6 yield. These experiments are, in fact, not as straightforward as intended because the extent of decomposition f, and therefore $[CF_3]_o$, are temperature dependent as well, as is the

reaction. The variation of f with temperature is shown in the inset in Figure 7a. Thus, these experiments were performed under conditions where $[CF_3]_0$ and T_{SiO_2} were both changing and affecting reaction rates.

<u>CF_3 Recombination and k_w</u>

As we pointed out in the Experimental section, k_w, the net surface loss of CF_3 may be obtained from C_2F_6 yields via equation (5). In effect, this method of obtaining k_w corresponds to measuring the extent to which C_2F_6 formation departs from purely second-order behaviour with respect to CF_3. The discrepancy is caused by CF_3 escape and surface loss, both of which are first-order. Knowledge of k_r[15] (recombination) and k_e (escape) allow the determination of k_w.

Figure 8a shows the C_2F_6 results of Figure 3 plotted in the form of equation (5). These data conform nicely to expression 5, giving linear plots with intercept 2.0 for all the temperatures studied. Table II summarizes the information obtained from these results. k_w is obtained from the slopes, using $k_r = 3.3 \times 10^{-12}$ cm^3 s^{-1}* and k_e in expression (5). Notice that k_w increases with increasing surface temperature indicating that increasing amounts of CF_3 are irreversibly lost in the surface reaction. An Arrhenius plot of $\ell n\, k_w$ versus the reciprocal surface temperature is shown in Figure 8b, together with a least-squares fit. The resulting k_w is given by the following expression: $k_w = 10^{2.9} \exp(-4700/RT)$ s^{-1}, where R = 1.987 cal mol^{-1} K^{-1}.

---

*k_r used in evaluating k_w was taken independent of the surface temperature because it is a gas phase reaction, whose temperature is governed by that of the vessel walls. Since the hot active surface constitutes only 5% of the reactor walls, the correction would be small. Furthermore, the dependence of k_r on temperature is not very strong in this range.

Having determined k_w, we now know all of the rate constants in scheme 1-4, and therefore can obtain the steady-state CF_3 concentration:

$$[CF_3]_{ss} = \frac{-(k_e + k_w) + \left((k_e + k_w)^2 + 2k_r f F^i_{CF_3I} V^{-1}\right)^{1/2}}{4 k_r} \qquad (6)$$

We find that $[CF_3]_{ss}$ is between 5-20% of $[CF_3]_o$ for the temperature range studied.

Formation of CO and k_{CO}

We have chosen the formation of CO as a marker for of the surface reaction of CF_3 with H_2O. Figure 9 shows the data in Figure 5 plotted as [CO] versus the steady-state CF_3 concentration, $[CF_3]_{ss}$. For all the temperatures, [CO] is linear with respect to $[CF_3]_{ss}$ and has no intercept, indicating a first-order reaction as would be expected from equation (4). The observed CO formation rate constant k_{CO} is obtained from the slope in each case (slope = k_{CO}/k_e^{CO}) ; these are given in Table 2. The resulting k_{CO} can be represented by the following Arrhenius expression: $k_{CO} = 10^{3.7} \exp(-7500/RT)\ s^{-1}$ (Figure 9b).

Notice in Table 2 that the k_{CO} rate constants are smaller than the corresponding k_w based on the loss of CF_3 on the heated fused silica surface. The latter indicates that not all the CF_3 that is lost to the surface from the gas phase (reaction 4) proceed to form CO. This results in an apparent excess of CF_3 on the surface, which must be removed by some other reaction.

The simplest mechanism that accommodates these results replaces equation (4) with equations (4a,b,c):

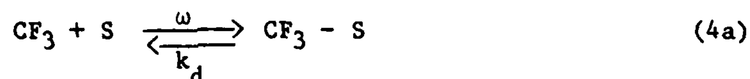

$$CF_3 + S \underset{k_d}{\overset{\omega}{\rightleftharpoons}} CF_3 - S \qquad (4a)$$

$$CF_3 - S \xrightarrow{k_1} CO \qquad (4b)$$

$$CF_3 - S \xrightarrow{k_2} \text{other products} \qquad (4c)$$

Equation (4a) represents adsorption and desorption of CF_3 where ω is the collision frequency of CF_3 with the active surface and k_d is the rate constant for desorption. (4b) represents the formation of CO, and (4c) corresponds to the sum of all those reactions that make up for the CO deficiency. The experimentally observed quantities k_w and k_{co} may be expressed in terms of mechanism (4a-c) as follows:

$$k_w = \frac{\omega\,(k_1 + k_2)}{(k_d + k_1 + k_2)} \qquad (7)$$

$$k_{CO}\text{ (observed)} = \frac{\omega\, k_1}{(k_d + k_1 + k_2)} = \frac{k_1}{(k_1 + k_2)}\, k_w \qquad (8)$$

Using our measured k_{CO} and k_w, we obtain for the branching ratio, $\frac{k_1}{(k_1 + k_2)} = 10^{0.8} \exp(-2800/RT)$. In relation to our experiments, equation (4c) may include the observed products CO_2 and COF_2. However, the latter can account for only 10% of the CO deficiency. Of course, (4c) may include reactions generating involatile products on the surface; these would not be determined by gas-phase analysis.

CF_3 Sticking Coefficient on Fused Silica

γ, the sticking coefficient is given by k_w/ω where ω is the collision frequency of CF_3 with the silica surface. γ is the probability that a CF_3 impinging on this surface will be irreversibly lost. The values obtained for γ are listed in Table II. Notice that these are low, between 0.0014-0.017 depending on the temperature, in contrast to values in the literature, measured as 0.08-0.75 for CF_3 on silicon at room temperature.[16] In our case, a close-to-unity γ would have implied that the surface loss of CF_3 were competitive with ω. Since $\omega \sim 600\ s^{-1}$ and the time scale for gas-phase chemistry is in the order of seconds, negligible gas-phase reaction (i.e., recombination) would have been expected under conditions where $\gamma \sim 1$ and $k_w \sim \omega$. Our results indicate that this is not the case.

As a further test to confirm that γ is not close to unity, we carried out experiments where the gas-phase CF_3 radicals were trapped by Cl_2, yielding CF_3Cl. The resulting product yields versus Cl_2 flow rate are shown in Figure 10. Notice that the surface reaction yielding CO is competitive with the gas-phase trapping reaction yielding CF_3Cl. Furthermore, behavior of the surface product CO resembles that of the gas-phase recombination product C_2F_6. That surface chemistry competes with gas-phase chemistry indicates once again that the surface reaction is slow compared to ω and that $\gamma \ll 1$.

The competition between the trapping reaction and the surface reaction may be seen more clearly by adding the trapping reaction (9) to the scheme depicted by equations (1) - (4a-c).

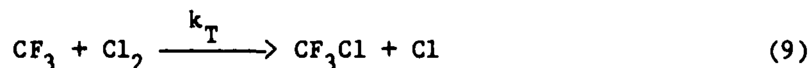

$$CF_3 + Cl_2 \xrightarrow{k_T} CF_3Cl + Cl \quad (9)$$

Equation (9) represents one more loss process for the CF_3 radicals formed in the reactor, in addition to recombination, escape and surface loss. The rate of loss of CF_3 radicals from the gas-phase, $k_{loss}^{CF_3}$, is given by

$$k_{loss}^{CF_3} = k_T\,[Cl_2] + k_r[CF_3] + k_e + \gamma\omega \qquad (10)$$

Notice in Equation (10) that the homogeneous Cl_2 trapping reaction is in direct competition with the CF_3 surface loss $\gamma\omega$, as well as with escape (k_e) and recombination ($k_r[CF_3]$). Varying $[Cl_2]$ allows for varying degrees of competition, as seen in Figure 10. Notice that even a small concentration of Cl_2 affects both the recombination product C_2F_6 and the surface reaction product CO. The fact that the surface product yield is reduced by such a small amount of Cl_2 indicates that trapping by Cl_2 and the surface reaction are competitive, leading to $\gamma \ll 1$. Although the data shown in Figure 10 may be modeled by including reaction (9) in our earlier reaction scheme, this will have to wait for reliable values of k_T. However, the trapping experiments demonstrate the usefulness of our approach for obtaining γ.

The present study reveals that the major reactivity of CF_3 radicals on the silica surface is with H_2O and not with SiO_2. Under these conditions, where H_2O is always present on the surface, the CF_3 + SiO_2 reaction accounts for only ~ 1% of the reactivity of CF_3 with H_2O. Added water inhibits the CF_3 + SiO_2 etching reaction even further. This is an important result that may be significant in applications. For example, presence of water in plasma etching systems may inhibit etching by radicals and may affect the final results. In the future, we plan to eliminate water in our experiments by using

a stainless steel reactor and will then direct our attention to the CF_3 + SiO_2 reaction as well as other etching reactions.

It should be mentioned that we also investigated the reaction between CF_2 radicals and the SiO_2 surface. These were hot-wire experiments where CF_2HCl was decomposed, yielding CF_2 radicals. By contrast to our work with CF_3, we did not see any SiF_4, nor any other surface-related products in the CF_2 experiments. This result is in contrast to those of Brannon,[8] and of Loper and Tabat[4] who found that CF_2 radicals etched SiO_2 considerably while etching by CF_3 was not observed. In their experiments, the surface as well as the gas was irradiated. Recent results of Brannon[17] indicate that when the surface is not irradiated, CF_2 radicals do not etch SiO_2, but rather deposit onto the surface as a fluorocarbon layer. The latter results are compatible with our findings for CF_2. The fact that etching by CF_3 was not observed by either of the above mentioned workers may seem to contradict our results for CF_3. However, we suspect that under the experimental conditions of those studies, there may have been a negligible concentration of CF_3 radicals. In the case of Brannon's study[8], CF_3 radicals were produced in a focussed beam and the high intensities may have led to secondary decomposition of CF_3. In the work of Loper and Tabat[4], where high pressures (50-100 Torr) were employed, it is possible that second-order recombination yielding C_2F_6 consumed most of the CF_3 radicals, so that etching by CF_3 was not observed.

Our results demonstrate that the VLPΦ method may be successfully used to study radical-surface reactions. Not only qualitative information on gas-phase products, but also quantitative information on the reaction kinetics may be obtained. The technique allows for determination of the order of the surface reaction, the rate constant and its temperature dependence, and also, k_w, the

surface loss constant for the reactive radical. Knowledge of k_w leads directly to γ, the sticking coefficient for the radical of interest.

In future experiments, we plan to extend the technique to include in situ detection of radicals by multiphoton ionization. This will allow for the determination of local real-time concentrations of radicals within the reactor. In addition to gas-phase product analysis, we also plan to probe the surface using surface analysis techniques, such as SALI (Surface Analysis by Laser Ionization) recently developed at SRI.[18]

REFERENCES

1. J. W. Coburn, Plasma Chemistry and Plasma Processing, 2, 1 (1982).

2. D. L. Flamm, V. M. Donnelly, and D. E. Ibbotson, J. Vac. Sci. Technol., B, 1, 23 (1983).

3. J. W. Coburn and H. F. Winters, J. Vac Sci. Technol., 16, 391 (1979).

4. G. L. Loper and M. D. Tabat, Proceedings of the International Conference on Lasers '83, R. C. Powell, ed., STS Press, McLean, VA, 1983.

5. D. L. Flamm, C. J. Mogab, and E. R. Sklaver, J. Appl. Phys., 50, 6211 (1979).

6. H. F. Winters and F. A. Houle, J. Appl. Phys., 54, 1218 (1983).

7. G. L. Loper and M. D. Tabat, Appl. Phys. Lett., 46, 654 (1985).

8. J. H. Brannon, J. Phys. Chem., accepted.

9. J. W. Coburn, H. F. Winters, and T. J. Chuang, J. Appl. Phys., 48, 3532 (1977).

10. S. C. McNevin and G. E. Becker, J. Vac. Sci. Technol., B, 2, 27 (1984).

11. M. J. Rossi, J. R. Barker, and D. M. Golden, J. Chem. Phys., 71, 3722 (1979).

12. D. M. Golden, M. J. Rossi, A. C. Baldwin, and J. R. Barker, Acc. Chem. Res., 14, 56 (1981).

13. M. J. Rossi and D. M. Golden, Int. J. Chem. Kinetics, 15, 1283 (1983).

14. A. C. Baldwin and D. M. Golden, J. Geophys. Res., 85, 2888 (1980).

15. k_r, the gas-phase CF_3 recombination rate constant, was investigated in separate experiments. These were performed using the same VLPΦ reactor, but in the absence of the active fused silica surface. Measurements with two sizes of escape apertures allowed the determination of k_r, as well as possible loss, k_w, on the gold-coated walls. These yielded $k_r = 3.3 \times 10^{-12}$ cm^3 s^{-1} and very small wall loss $k_w \sim 0.04$ s^{-1}. This study of homogeneous CF_3 recombination will be presented in a forthcoming paper.

16. H. F. Winters, J. Appl. Phys., 49, 5165 (1978).

17. J. H. Brannon, private communication.

18. C. H. Becker and K. T. Gillen, Anal. Chem., 56, 1671 (1984).

Table 1

OXYGEN-ISOTOPE ABUNDANCES OF PRODUCTS
CO, CO_2, AND COF_2 IN HOT-WIRE EXPERIMENTS WITH H_2O^{18}.*

Species	H_2O^{16}	H_2O^{18}	CO^{16}	CO^{18}	$CO_2{}^{16}$	$CO^{16}O^{18}$	$CO_2{}^{18}$	$CO^{16}F_2$	$CO^{18}F_2$
m/e	18	20	28	30	44	46	48	47	49
S(mV)	3.92	4.55	2.8	3.0	0.20	0.48	0.26	0.04	0.04
Ratio	1.0 :	1.16	1.0 :	1.07	1.0 :	2.4 :	1.3	1 :	1

---

*$F^{i}_{H_2O^{18}} \cong 1.0 \times 10^{15}\ s^{-1}$.

$T_{SiO_2} = 100°C$.

$F^{i}_{CF_3I} = 1.4 \times 10^{15}\ s^{-1}$.

(Increasing $F^{i}_{CF_3I}$ from 1.4×10^{15} to $8.2 \times 10^{15}\ s^{-1}$ increased the product yields but did not change the isotopic ratios.)

Table 2

k_w, k_{CO}, and γ AS FUNCTIONS OF T_{SiO_2}

T_{SiO_2}(C)	k_w (s^{-1}) *	k_{CO} (s^{-1})**	γ +
70	0.85	0.103	0.0014
160	2.79	0.401	0.0047
205	5.87	2.16	0.0098
260	10.1	3.84	0.017

*Obtained from slopes in Figure 8a using equation 5.

**Obtained from Figure 9a; slope = k_{CO}/k_e^{CO}.

+$\gamma = k_w/\omega$ where $\omega = 600\ s^{-1}$ for CF_3 collisions with the silica surface.

FIGURE CAPTIONS

Figure

1 Low-Pressure Photolysis Cell for the Investigation of Free Radical-Surface Interactions.

The 2-inch diameter fused-silica flat lies horizontally in the wafer compartment.

2 Mass Spectometric Data from Laser Experiments.

Pulse repetition rate = 20 Hz. $F^{i}_{CF_3I} = 8 \times 10^{15}\ s^{-1}$.

$T_{SiO_2} = 230°C$. The figure shows signals as functions of time as laser is turned on and off.

3 Effect of Water on Products in Hot-Wire Experiments.

(a) SiF_4 signal at 85 m/e. $F^{i}_{CF_3I} = 1.1 \times 10^{15}\ s^{-1}$;

$F^{i}_{D_2O} \cong 3 \times 10^{15}\ s^{-1}$; $T_{SiO_2} = 145°C$.

(b) CO signal at 28 m/e. Other conditions given in (a).

(c) C_2F_6 signal at 119 m/e. $F^{i}_{CF_3I} = 1.4 \times 10^{15}\ s^{-1}$;

$F^{i}_{H_2O^{18}} \cong 1 \times 10^{15}\ s^{-1}$; $T_{SiO_2} = 100°C$.

4 $[C_2F_6]$ as a Function of $[CF_3]_o$ for Laser Experiments at Various Substrate Temperatures.

$[CF_3]_o$ was varied by changing $F^{i}_{CF_3I}$ from 1×10^{15} to $1 \times 10^{16}\ s^{-1}$.

5 [CO] as a Function of $[CF_3]_o$ for Various Substrate Temperatures.

Conditions same as in Figure 4.

6 $[SiF_4]$, $[CO_2]$, and $[COF_2]$ as Functions of $[CF_3]_o$ for T_{SiO_2} = 260°C. Conditions same as in Figure 4.

7 Product Concentrations as Functions of T_{SiO_2} in Laser Experiments.

(a) CO, HF, and C_2F_6.

(b) COF_2, CO_2, and SiF_4.

The inset shows f, the fractional depletion in CF_3I as a function of T_{SiO_2}; see text for details. $F^i_{CF_3I} = 4.0 \times 10^{15}\ s^{-1}$.

8 (a) $f\ F^i_{CF_3I}\ /\ F^o_{C_2F_6}$ as a Function of $F^{o\ 1/2}_{C_2F_6}$ (see equation 5 in text). The straight lines correspond to least-squares fits to the data with intercept = 2.0.

(b) ln k_w as a Function of $T^{-1}_{SiO_2}$. The line is the linear least-squares fit, corresponding to $k_w = 10^{2.9} \exp(-4700/RT)$.

9 (a) [CO] as a Function of $[CF_3]_{ss}$.

$[CF_3]_{ss}$ was obtained using equation 6 (see text for details). The straight lines correspond to least-squares fits to the data with intercept 0.

(b) ln k_{CO} as a Function of $T^{-1}_{SiO_2}$.

The line is the linear least-squares fit corresponding to $k_{CO} = 10^{3.7} \exp(-7500/RT)$.

10 Mass Spectral Signals of Products CF_3Cl, CO, and C_2F_6 as Functions of Cl_2 Flow Rate for Trapping Experiments $F^i_{CF_3I} = 3.1 \times 10^{15}\ s^{-1}$, T_{SiO_2} = 110°C.

$[Cl_2](cm^{-3})$ is given by $4.1 \times 10^{-3} F^i_{Cl_2}(s^{-1})$.

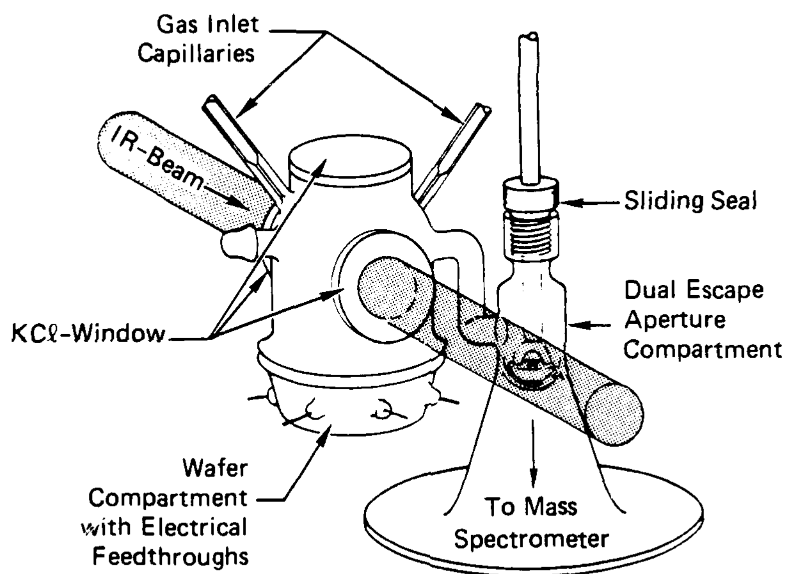
Gas Inlet
Capillaries
IR-Beam
Sliding Seal
Dual Escape
Aperture
Compartment
KCℓ-Window
Wafer
Compartment
with Electrical
Feedthroughs
To Mass
Spectrometer
JA-330583-375

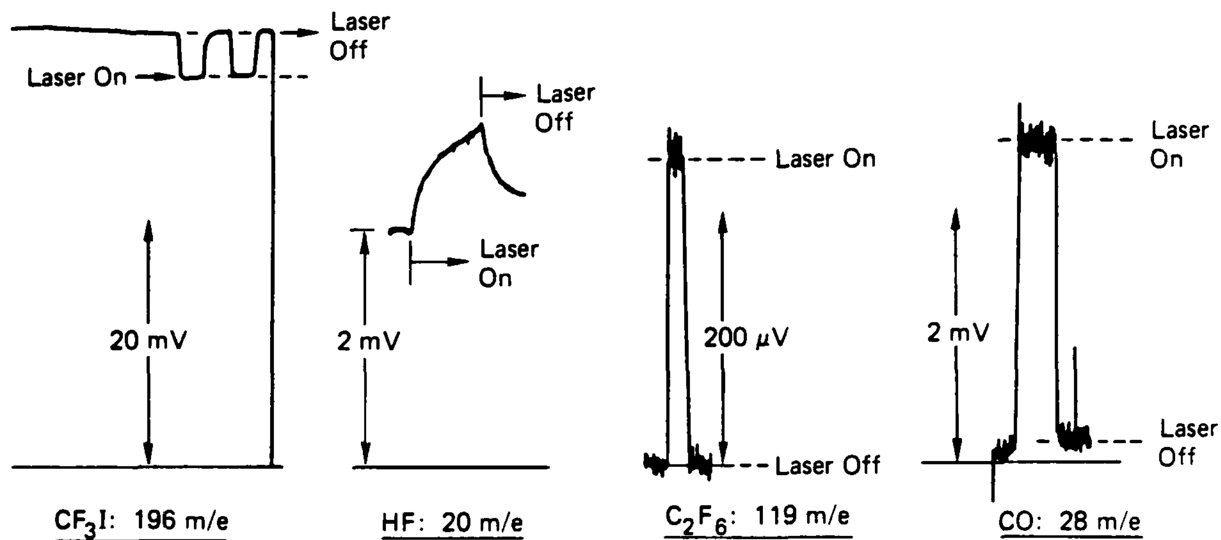

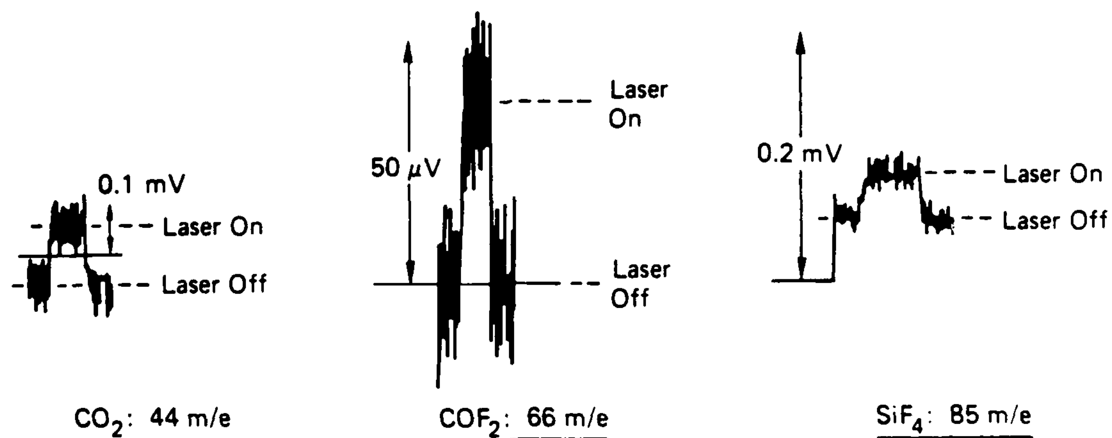

JA-7873-56A

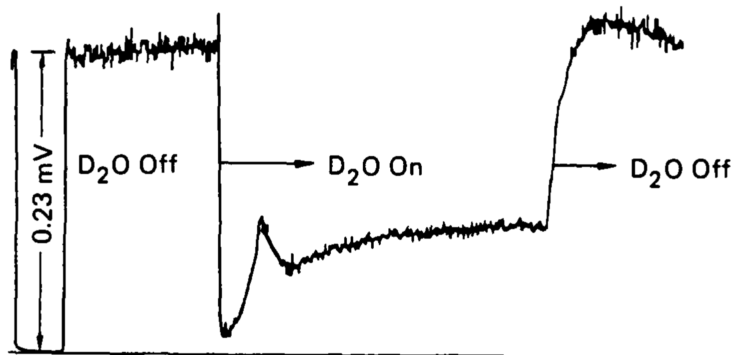

(a) SiF_4

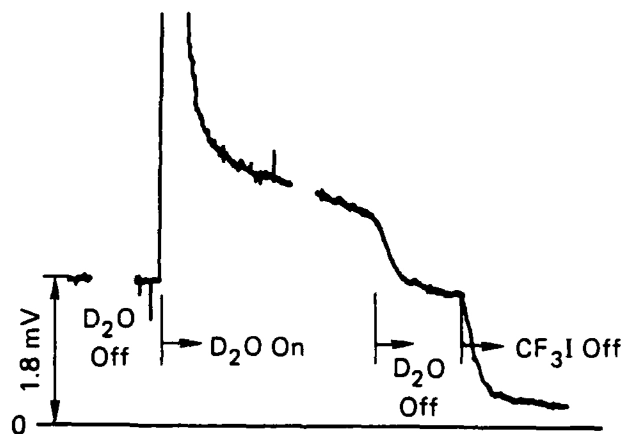

(b) CO

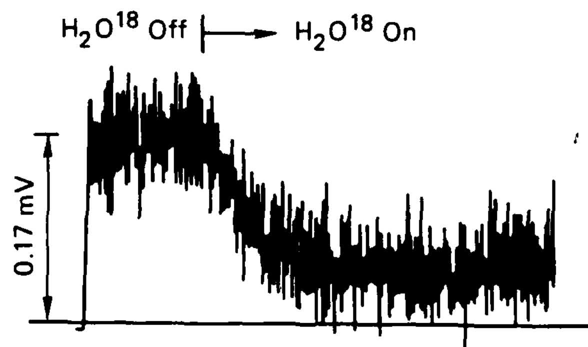

(c) C_2F_6

JA-7873-57A

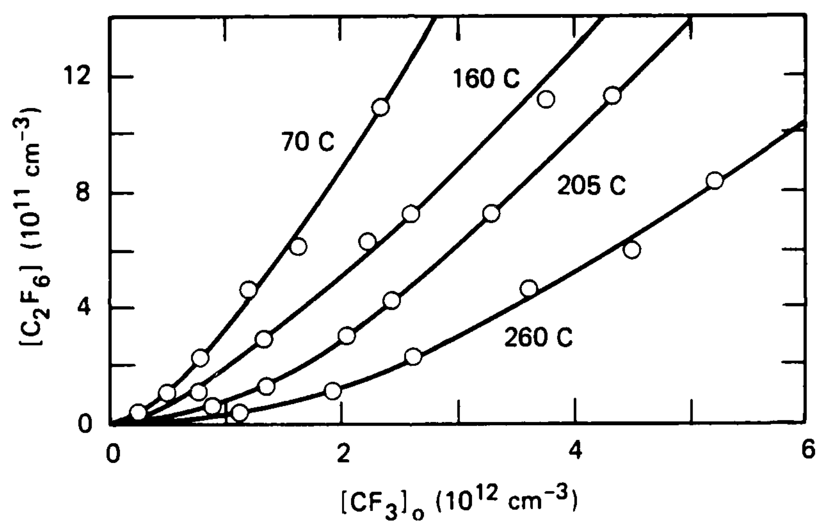

12
8
4
0
$[C_2F_6]$ $(10^{11}\ cm^{-3})$
70 C
160 C
205 C
260 C
0
2
4
6
$[CF_3]_o$ $(10^{12}\ cm^{-3})$
JA-4917-8

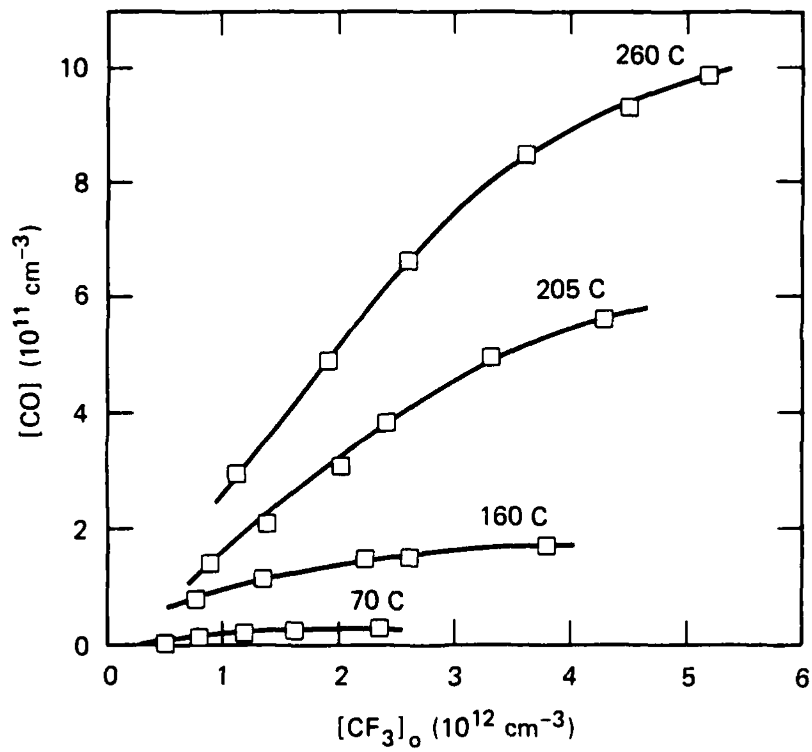

260 C
205 C
160 C
70 C
10
8
6
4
2
0
[CO] (10^{11} cm^{-3})
0
1
2
3
4
5
6
$[CF_3]_o$ (10^{12} cm^{-3})
JA-4917-9

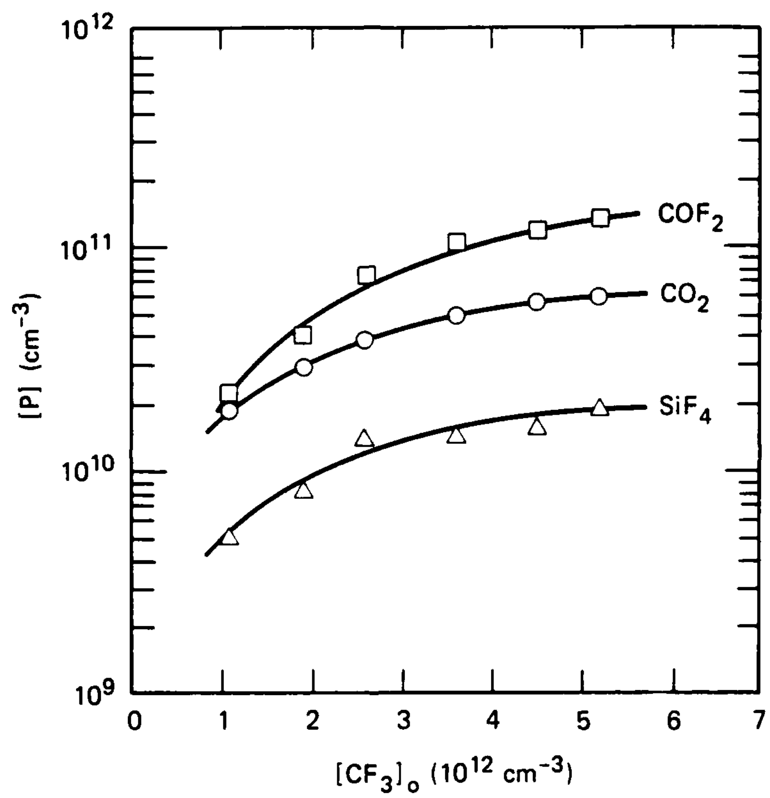
10^{12}
10^{11}
10^{10}
10^{9}
[P] (cm^{-3})
COF_2
CO_2
SiF_4
0
1
2
3
4
5
6
7
$[CF_3]_o$ (10^{12} cm^{-3})
JA-4917-10

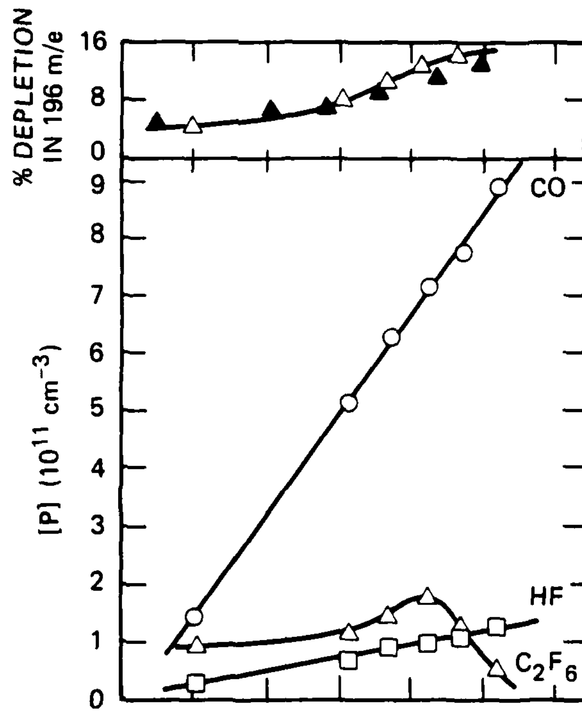

(a)

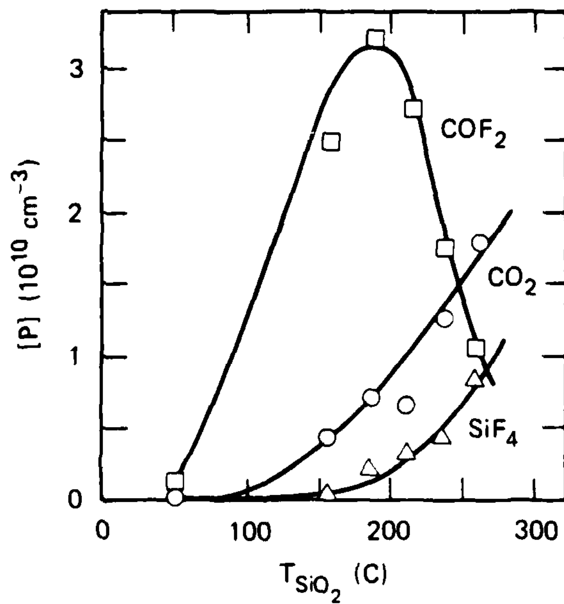

(b)

JA-4914-11

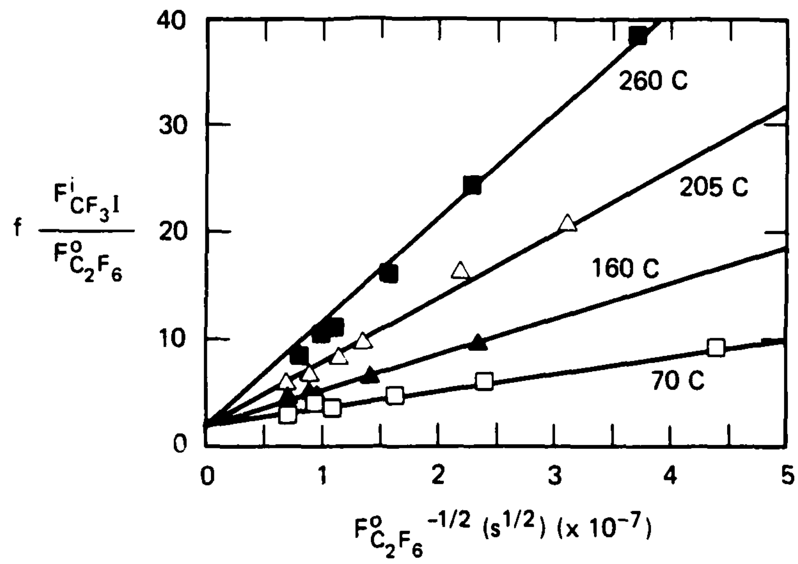

(a)

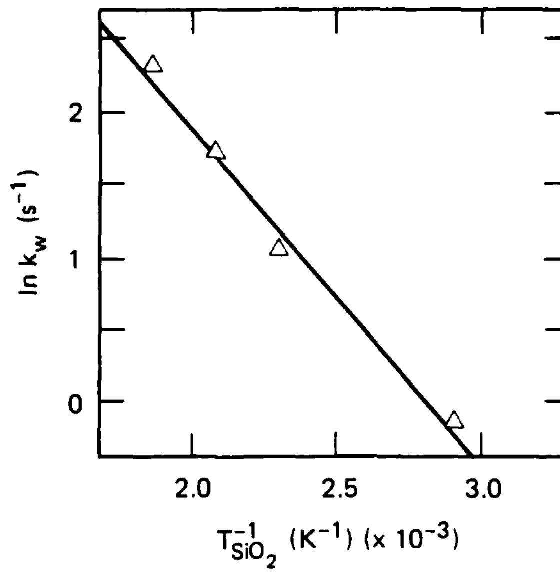

(b)

JA-4917-12

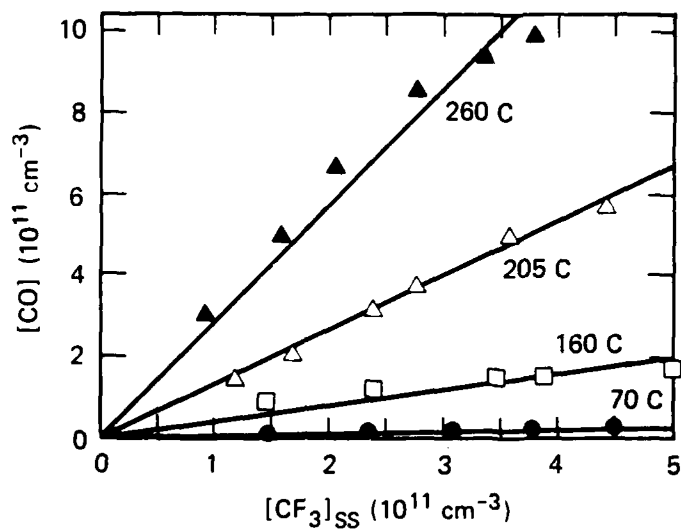

(a)

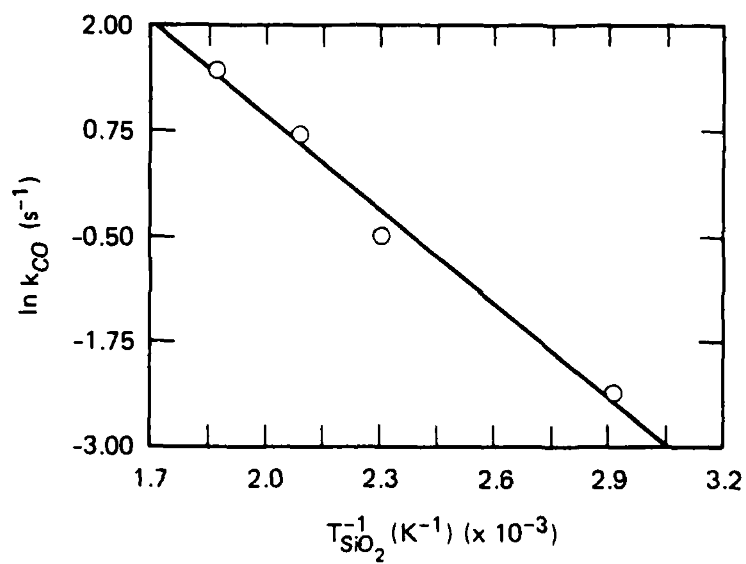

(b)

JA-4917-13

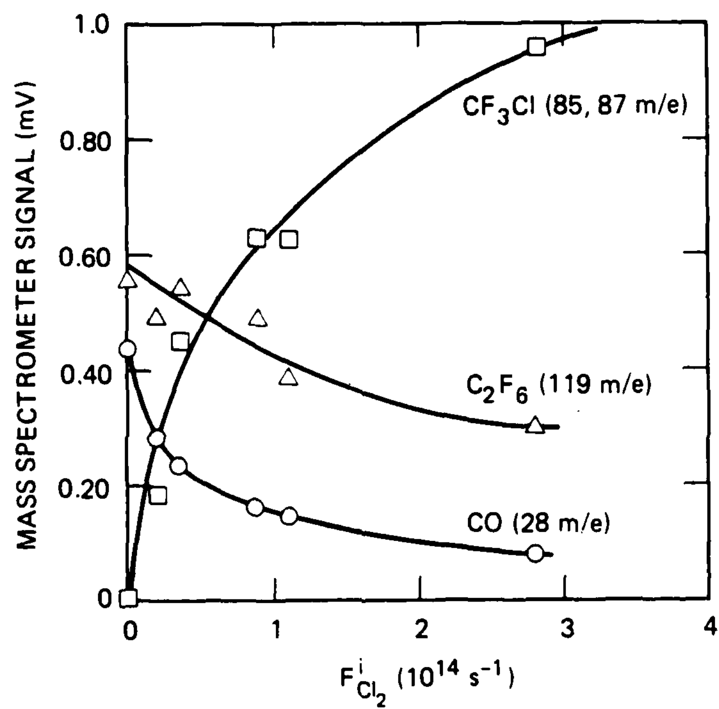

MASS SPECTROMETER SIGNAL (mV)
1.0
0.80
0.60
0.40
0.20
0
0
1
2
3
4
$F^{i}_{Cl_2}$ (10^{14} s^{-1})
CF_3Cl (85, 87 m/e)
C_2F_6 (119 m/e)
CO (28 m/e)
JA-4917-14

Appendix C

ABSOLUTE RATES OF RECOMBINATION OF CF_3 RADICALS

By: N. Selamoglu, M. J. Rossi, and D. M. Golden

Accepted by Chemical Physics Letters

ABSOLUTE RATE OF RECOMBINATION OF CF_3 RADICALS

N. Selamoglu,[†] M. J. Rossi, and D. M. Golden
Department of Chemical Kinetics
SRI International, Menlo Park, CA 94025

ABSTRACT

The homogeneous rate of recombination of CF_3 radicals at 300K was studied in a VLPΦ flow reactor. The radicals were generated from CF_3I by either CO_2 laser (1076 cm^{-1}) or excimer laser (248 nm) photolysis. The precursor and product concentrations were followed by mass spectrometry. The recombination rate constant, k_r, was measured as 3.0 (∓0.4) x 10^{-12} cm^3 s^{-1}. A hindered Gorin transition-state model predicts that k_r/k_r^{∞} is only 0.74 at the effective pressures employed. The model was used to fit these experiments at 300 K, as well as earlier experiments at ~ 1000 K.

*This work was supported by the Air Force Office of Scientific Research under Contract No. F49620-83-K-0001.

[†]Postdoctoral Research Associate.

CK85-31

Recombination rates for radicals represent the basis on which many other radical reaction rates are studied.[1] Many radical-molecule metathesis and radical disproportionation reactions have been measured relative to radical recombination rates, so that there is a need for accurate recombination rate constant values. In the case of the CF_3 radical, which is prototypical for the important class of perfluorinated alkyl radicals, there is a substantial uncertainty in the rate constant for recombination.[2-7] Also, recent interest in quantitative understanding of plasma etching serves as an additional reason for pursuing the correct value for k_r.[8]

The rate constant for CF_3 recombination, k_r, has been measured near room temperature by various workers using different techniques.[2-5] These values show almost an order of magnitude variation, ranging from about 5×10^{-12} to 4×10^{-11} cm^3 s^{-1} in the temperature range 300-400 K where all correspond to the high pressure limit. At higher temperatures (900-1100 K) CF_3 recombination was studied in this laboratory[6] by the VLPP (Very Low Pressure Pyrolysis) flow method, under conditions corresponding to falloff where $k_r \sim 10^{-13}$. In addition, at 1300 K, k_r has been measured as 3.2×10^{-11} cm^3 s^{-1} in a shock-tube study.[7]

The large discrepancy among the low-temperature measurements prompted us to measure k_r absolutely using the VLPΦ (Very Low-Pressure Photolysis) technique. The latter method derives from VLPP, which has been successfully used for the measurement of various radical recombination rates.[6,9,10] Our present measurements at room temperature together with our earlier data on CF_3 recombination at ~ 1000 K provide rate constants over a wide temperature range.

The experimental method has been described in detail previously.[11,12] In short, the VLPΦ technique utilizes a dual-aperture low-pressure (<10 mTorr) Knudsen flow reactor, where molecular flow conditions are maintained. The radical precursor CF_3I flows through the reactor where it yields CF_3 radicals via photodecomposition. Either CO_2 infrared-multiphoton excitation or UV-excimer laser excitation was used in the present study. The CF_3 radicals reside in the reactor for 0.5-1.0 s, depending on the escape aperture size, during which time recombination occurs. The number of wall collisions of CF_3 during its residence time is 1.3×10^4 (for small aperture) and 6.8×10^3 (for large aperture), ensuring that radicals, which may be formed hot, thermalize to the wall temperature before reacting. The laser-pulse repetition rates were chosen so that nearly steady-state conditions prevailed in the reactor; i.e., the time between pulses (0.01-0.05 s) << typical residence times (0.5-2.0 s). Reactants and products form an effusive molecular beam at the reactor exit which is chopped by means of a tuning-fork chopper and analyzed using a Balzers 311 quadrupole mass spectrometer. The technique discriminates against background gases not originating from the cell.

Experiments consisted of flowing CF_3I through the reactor, and measuring steady-state mass spectrometric signals of CF_3I (196 m/e) and C_2F_6 (119 m/e) with laser on/off. The fractional decrease in CF_3I with the laser irradiation, f, is a direct measure of the CF_3 radical yield. Measurements were carried out as functions of CF_3I flow rate for both sizes of the escape aperture.

The parameters for the VLPΦ reactor are: $V = 250$ cm^3; reactor wall area = 420 cm^2; IR or UV beam pathlength = 10 cm. The escape rate constant, $k_e(M)$, for species with molecular weight, M, is given by $0.475\ (T/M)^{1/2}$ and 0.887

$(T/M)^{1/2}$ for the small and large apertures, respectively. The wall collision frequency is given by $\omega = 6132\ (T/M)^{1/2}$. The pyrex reactor was gold-coated (Engelhard Industries) to minimize wall losses. For the photodecomposition, either a Tachisto 555 CO_2 laser at 20 Hz (1076 cm^{-1}, 9.6 R16; 0.8 J cm^{-2} per pulse) or a Lumonics Hyperex 400 excimer laser at 100 Hz (248 nm; ~ 100 mJ cm^{-2} per pulse) was used, effecting 3-12 % fractional dissociation per pulse in the irradiation volume.

Competing processes involving the CF_3 radical in a VLPΦ reactor are described by

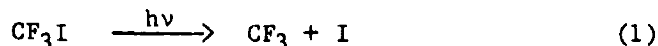

$$CF_3I \xrightarrow{h\nu} CF_3 + I \qquad (1)$$

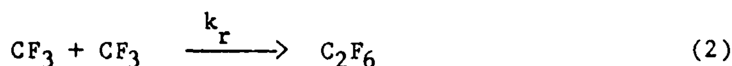

$$CF_3 + CF_3 \xrightarrow{k_r} C_2F_6 \qquad (2)$$

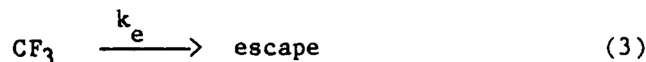

$$CF_3 \xrightarrow{k_e} \text{escape} \qquad (3)$$

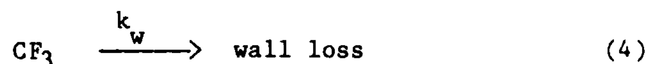

$$CF_3 \xrightarrow{k_w} \text{wall loss} \qquad (4)$$

where (1) represents the laser decomposition of CF_3I and (2) is the recombination reaction of interest. (3) represents the effusion of CF_3 out of the reactor and (4) describes possible first-order loss of CF_3 on the reactor walls. The basis for the method is the competition between first-order CF_3 losses (3) and (4) and second-order recombination (2). Under steady-state conditions, the above scheme leads to the following expression

$$f(F^{i}_{CF_3I})/(F^{o}_{C_2F_6}) = 2 + (k_e + k_w)k_r^{-1/2}\ V^{1/2}\ F^{o}_{C_2F_6}{}^{-1/2} \qquad (5)$$

where $F^{i}{}_{CF_3I}$ is the flow rate of CF_3I into the reactor, $F^{o}{}_{C_2F_6}$ is the C_2F_6 flow rate out of the reactor, V is the volume and f is the fractional depletion in the steady-state CF_3I signal when the sample is irradiated. Expres-

sion (5) allows for the determination of k_r and k_w, with the appropriate measurements.

Figure 1 shows a representative set of experimental data plotted in the form of equation (5). The two groups of data correspond to two different sizes for the escape aperture. Notice that both groups of data are linear, as expected from expression (5), and indicate an intercept close to 2.0. The solid lines represent linear least-squares fitting of the data, where the intercept was constrained to 2.0. From the slopes of the two data groups, where each slope corresponds to $(k_e + k_w)k_r^{-1/2} V^{1/2}$, k_r and k_w may be obtained.

k_r and k_w values obtained from Figure 1 and from other similar data sets are collected in Table 1. Notice that the recombination rate constant, k_r, is between 2.19×10^{-12} and 3.35×10^{-12} $cm^3\ s^{-1}$. Also shown in the table for comparison are values obtained, k_r', when the least-squares fitting was not forced through intercept 2.0. These k_r' are reasonably close to k_r. Also notice that k_r from experiments 1, 2, and 4, in which CF_3 radicals were generated by CO_2 laser multiphoton decomposition, agree very well with experiment 3, where the radicals were generated via KrF excimer-laser photolysis. This demonstrates that the method used to create the radicals does not affect the subsequent kinetics of CF_3. The radicals are thermalized at the walls to room temperature before they react, as expected.

k_w is the observed rate constant for the net first-order loss of CF_3 on the reactor walls. For entries 1-3 in Table 1, k_w is rather small, between 0.02-0.07 s^{-1}, when compared to k_e of 0.99 or 1.85 s^{-1} for the small and large apertures, respectively. The fact that the first-order wall loss of CF_3 is small compared to its first-order escape loss indicates the gold coating used

Table 1

EXPERIMENTAL RESULTS FOR k_r and k_w

Experiment Number	Excitation Laser	k_r ($cm^3\ s^{-1}$)*	k_w (s^{-1})	k_r' ($cm^3\ s^{-1}$)**
1	CO_2	2.19×10^{-12}	0.035	1.92×10^{-12}
2	CO_2	3.05×10^{-12}	0.023	6.00×10^{-12}
3	KrF Excimer	3.16×10^{-12}	0.066	3.13×10^{-12}
4	CO_2	3.35×10^{-12}	0.99	3.85×10^{-12}
		3.0×10^{-12}		

*Errors in individual determinations of k_r are $\approx 0.3 \times 10^{-12}$ (from standard deviations in least-square slope).

**k_r' refers to the recombination rate constant determined from the data when the least-square fitting intercept was not constrained to 2.0 (see text).

in the reactor is very efficient, leading to little CF_3 adsorption. Entry 4 in the table corresponds to an experiment where an uncoated fused silica flat with surface area corresponding to ~5% of the wall area was placed inside the reactor. The higher value of k_w for that experiment reflects the tendency of CF_3 to stick to silica surfaces.[13,6] Although some CF_3 does adsorb on the silica surface, it does not prevent measurements of the gas-phase recombination rate. Furthermore, the fact that k_r for this set, 3.35×10^{-12}, is close to the other sets indicates that presence of the silica in the reactor does not lead to heterogeneous recombination. Otherwise, a higher k_r would have been obtained in experiment (4).

In principle, the k_r obtained in these measurements correspond to the rate constant in its falloff, at the effective pressure of a VLPΦ reactor. The latter is governed by the gas-wall collision frequency in the reactor, as well as the gas-gas collision frequency. In order to assess the degree of falloff in our experiments, and compare our k_r measurements with k_r^∞ in the literature, RRKM calculations were carried out. These calculations also reveal the compatability of our room temperature measurements with earlier high-temperature measurements from this laboratory.

RRKM calculations were carried out for C_2F_6 decomposition using a hindered Gorin model[6,9,14] for the transition state, giving the unimolecular decomposition rate constant k_d. In turn, k_r was obtained from k_d via the thermodynamic relationship, $K = k_r/k_d$, where the equilibrium constant K was computed from the thermochemistry for reaction (2).[15] A hindered Gorin (rotational) model was found to be a better representation of the reaction than a vibrational transition-state model in our earlier study on CF_3 recombination,[6] so that the vibrational model was not used in this study. In

the hindered Gorin model, the vibrations corresponding to bending of a CF_3 group relative to the C–C axis in the molecule are replaced by two CF_3 rotations in the transition state, each with axes normal to the C–C bond axis. These rotations are constrained from free rotations by a hindrance parameter, η (%). The η parameter is a measure of the hindrance between the two CF_3 groups as they rotate towards each other. The effect of parameter η in the model is to reduce the effective moment of inertia product $I_1 I_2$ of each CF_3 rotor by

$$I_{eff} = I_1 I_2 \ (100-\eta)/100 \qquad (6)$$

In addition, the torsion around the C–C axis of threefold symmetry in the molecule is replaced by a free internal rotation in the transition state. The external rotation around the C–C axis is taken to be active. Zero activation energy was assumed for the recombination at 0 K so that the critical energy for bond breaking was set equal to $-\Delta E_o^{\,o}$ for reaction (2). The parameters used in the model calculations are given in Reference 6.

The experimental k_r at 300 K are shown in Figure 2 together with model results as functions of temperature. The solid curve represents k_r^∞ from the model while the dashed curve represents k_r under VLPΦ conditions. Also shown are experimental values for k_r^∞ around 300 K from the literature as well as our earlier VLPP results at T ~ 1000 K. Notice that the model with hindrance parameter η ~ 92% fits our present data at room temperature and our earlier data at ~ 1000 K reasonably well (dashed line).

Perhaps the most important result from the model is that the degree of falloff under our experimental conditions at 300 K is predicted to be very low, so that $k_r/k_r^\infty \sim 0.74$. This may be seen in Figure 2 by comparing the

dashed and solid lines at 300 K. Therefore, our present VLPΦ measurements should yield k_r very close to the high pressure limit. Notice, however, that our results represent a lower limit to the range of experimental data at 300 K. Even when the low pressure $k_r = 3 \times 10^{-12}$ is corrected to yield $k_r^\infty = 4 \times 10^{-12}$, this is still lower than the bulk of the literature data. In other words, the model that satisfactorily fits our VLPΦ data predicts k_r^∞ values lower than observed by other workers (compare literature data and solid line). The model cannot reconcile the difference between our data at room temperature and the spectrum of literature values for k_r^∞. The degree of falloff predicted by the model at room temperature, i.e., k_r/k_r^∞, is essentially insensitive to the degree of hindrance so that adjustment of the latter parameter does not eliminate the discrepancy. We can only conclude that some of the older values are inaccurate.[2,3,5]

The only high-temperature experimental study of CF_3 recombination is by Glänzer et al.,[7] yielding $k_r^\infty = 3.2 \times 10^{-11}$ cm^3 s^{-1} (1300 K), shown in Figure 2. This experimental value also lies above our model prediction of k_r^∞, as do lower temperature values. However, the disagreement is almost within the error bars given for the experimental k_r^∞ by the authors, as indicated in the figure. (The high-pressure limit to the rate constrant, k_r^∞, in Glänzer's work, was not measured directly, but was obtained by extrapolation from lower pressure shock-tube measurements.)

Although our data at the two extremes of temperature are fit very well by a constant $\eta = 92\%$, the data could easily accommodate a temperature-dependent η, changing from 92% to 98% as temperature increases from 300 K to 1000 K. η would be expected to increase with temperature on the basis that in the transition state, the centrifugal barrier moves to smaller C-C distances with

increasing temperature[14] and thereby increases the hindering effect between the two CF_3 groups. The latter leads to a decrease in k_r. We find that model k_r are rather sensitive to the value of η around 300 K, but less so at the higher temperatures. For example, changing η from 92% to 98% decreases k_r by a factor of 0.29 at 300 K, while the decrease at 1000 K is a factor of 0.65. On the logarithmic scale of Figure 2, and for 1000 K, model k_r with 98% hindrance would fall slightly below the model curve with η = 92%. However, not too much significance should be placed on the absolute value of η, which is dependent on transition-state parameters. For other recombination reactions,[9] η was found to be in the range ~ 60-99 %.

In summary, the CF_3 recombination reaction, under our conditions, appears to be a homogeneous gas-phase process, proceeding at the same rate regardless of whether or not an active silica surface is present in the cell. It was found that gold-coating of the vessel walls markedly eliminates CF_3 wall losses. The recombination reaction was found to be independent of the mode of excitation of the CF_3I precursor, indicating that hot CF_3 radicals do not play a role in the chemistry. Our VLPΦ determination of the CF_3 recombination rate yields $k_r = 3.0 \times 10^{-12}$ cm^3 s^{-1} at 300 K. These data, as well as earlier high-temperature rate constants, could be fit by a hindered Gorin model with η = 92%, yielding $k_r/k_r^{\infty} = 0.74$ at room temperature. k_r^{∞} (300 K) is computed as 4.0×10^{-12} from our $k_r = 3.0 \times 10^{-12}$ using k_r/k_r^{∞}.

References

1. Handbook of Bimolecular and Termolecular Reactions, J. A. Kerr and S. J. Moss, eds., Chemical Rubber Company, Boca Raton, 1981.

2. P. B. Ayscough, J. Chem. Phys., 24 (1956) 944.

3. T. Ogawa, G. A. Carlson, and G. C. Pimentel, J. Phys. Chem., 74 (1970) 2090.

4. N. Basco and F.G.M. Hathorn, Chem. Phys. Lett., 8 (1971) 291.

5. R. Hiatt and S. W. Benson, Int. J. Chem. Kinetics, 4 (1972) 479.

6. M. Rossi and D. M. Golden, Int. J. Chem. Kinetics, 11 (1979) 775.

7. K. Glänzer, M. Maier, and J. Troe, J. Phys. Chem., 84 (1980) 1681

8. D. L. Flamm and V. Donnelly, Plasma Chem. Plasma Proc. 1 (1981) 317

9. M. Rossi, K. D. King, and D. M. Golden, J. Am. Chem. Soc., 101 (1979) 1223.

10. K. Y. Choo, P. C. Beadle, L. W. Piszkiewicz, and D. M. Golden, Int. J. Chem. Kinetics, 8 (1976) 45.

11. M. J. Rossi, J. R. Barker, and D. M. Golden, J. Chem. Phys., 71 (1979) 3722.

12. D. M. Golden, M. J. Rossi, A. C. Baldwin, and J. R. Barker, Acc. Chem. Res., 14 (1981) 56.

13. N. Selamoglu, M. J. Rossi, and D. M. Golden, J. Chem. Phys., submitted.

14. (a) S. W. Benson, Thermochemical Kinetics, 2nd Ed., John Wiley and Sons, Inc., New York, 1976, p. 161.
    (b) S. W. Benson, Can. J. Chem., 61 (1983) 881.

15. JANAF Thermochemical Tables, NSRDS-NBS 37, U.S. GPO, Washington, D.C., 1970.

CAPTIONS

Figure

1 $f\ F^{i}_{CF_3I}/F^{o}_{C_2F_6}$ as a Function of $F^{o}_{C_2F_6}{}^{-1/2}$. (corresponds to Experiment (1) in Table 1).

△ large aperture, $k_e = 0.887\ (T/M)^{1/2}$

□ small aperture, $k_e = 0.475\ (T/M)^{1/2}$

The solid lines represent least-squares fitting of the data with intercept = 2.0.

2 k_r as a Function of Temperature.

△ This work

✕ Reference 6

○ Reference 4

◇ Reference 5

● Reference 3

□ Reference 2

▲ Reference 7

(- - - -) Model, VLPΦ conditions

(————) Model, k_r^{∞}

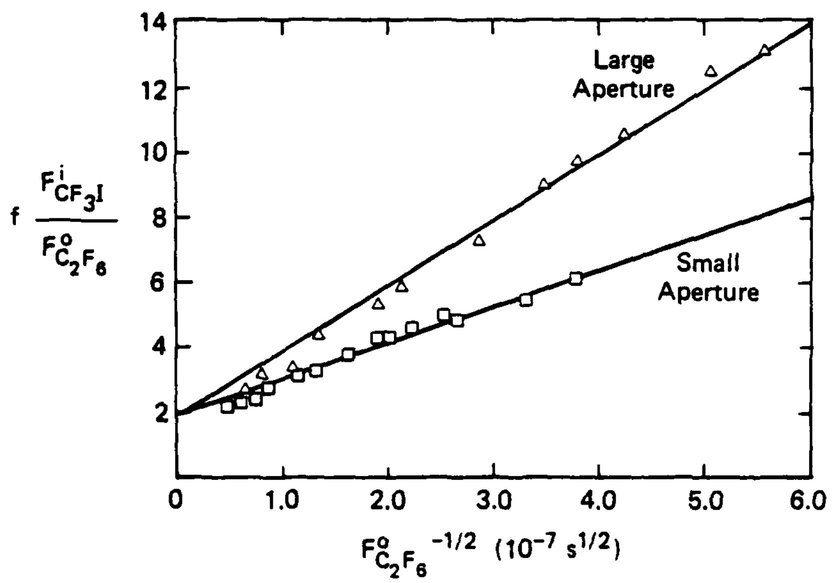

Large Aperture
Small Aperture
$f \frac{F^i_{CF_3I}}{F^o_{C_2F_6}}$
$F^o_{C_2F_6}{}^{-1/2}$ $(10^{-7}\ s^{1/2})$
0
1.0
2.0
3.0
4.0
5.0
6.0
2
4
6
8
10
12
14
RA-1227-1

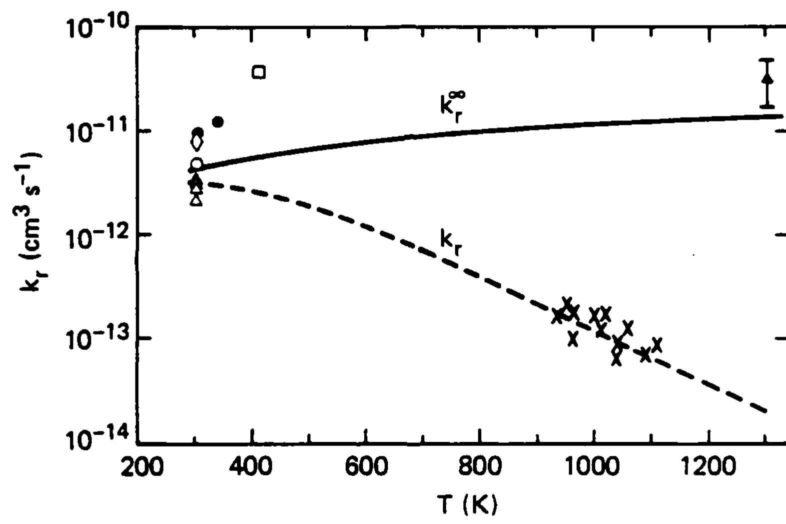
10^-10
10^-11
10^-12
10^-13
10^-14
k_r^∞
k_r
k_r (cm^3 s^-1)
200
400
600
800
1000
1200
T (K)
RA-1227-2

END

FILMED

1-86

DTIC